

Spectral relaxations of persistent rank invariants

With a focus on parameterized settings

Matt Piekenbrock[†] & Jose Perea[‡]

[†] Khoury College of Computer Sciences, Northeastern University

[‡]. Department of Mathematics and Khoury College of Computer Sciences, Northeastern University

Vectorizing diagrams

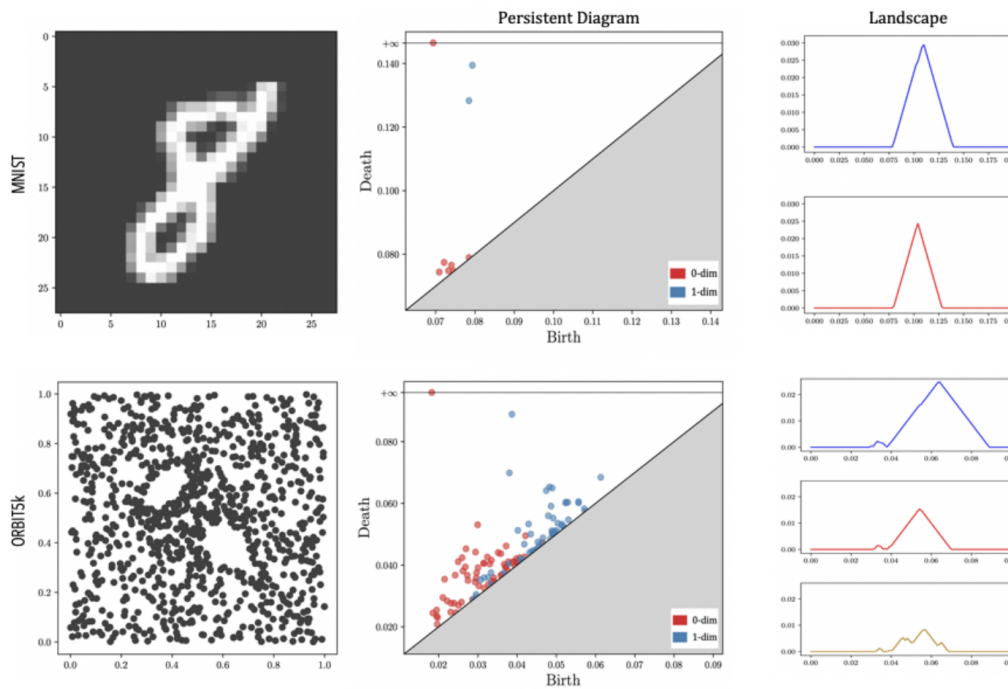
There are many mappings from dgm's to function spaces (e.g. Hilbert spaces)

- Persistence Landscapes ([Bubenik 2020](#))

Vectorizing diagrams

There are many mappings from dgm's to function spaces (e.g. Hilbert spaces)

- Persistence Landscapes ([Bubenik 2020](#)) + Learning applications ([Kim et al. 2020](#))



$$\lambda(k, t) = \sup\{h \geq 0 \mid \text{rank}(H_p^{i-h} \rightarrow H_p^{i+h}) \geq k\}$$

Vectorizing diagrams

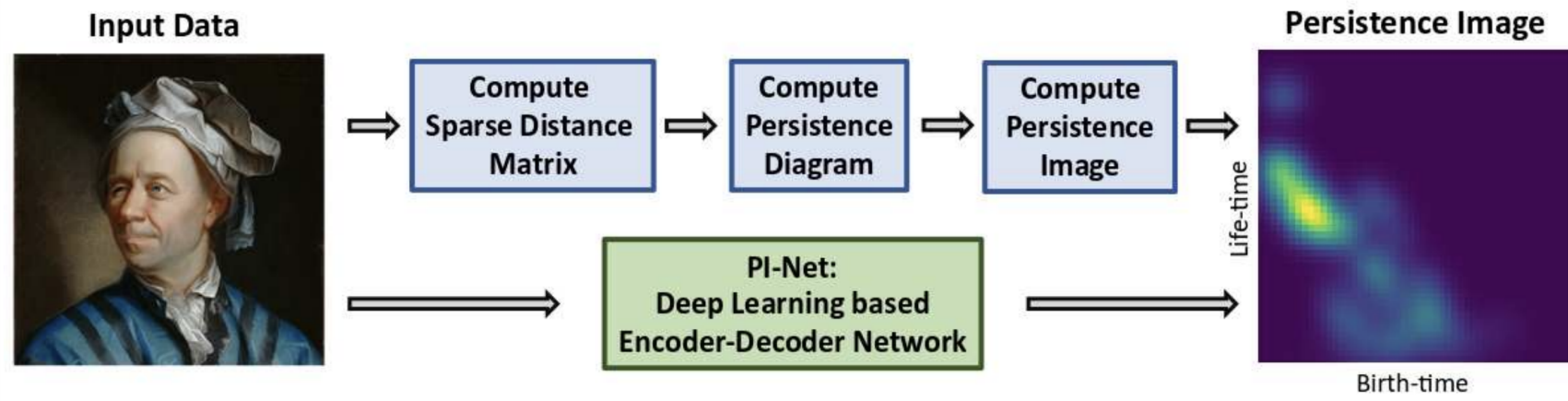
There are many mappings from dgm's to function spaces (e.g. Hilbert spaces)

- Persistence Landscapes ([Bubenik 2020](#)) + Learning applications ([Kim et al. 2020](#))
- Persistence Images ([Adams et al. 2017](#))

Vectorizing diagrams

There are many mappings from dgm's to function spaces (e.g. Hilbert spaces)

- Persistence Landscapes ([Bubenik 2020](#)) + Learning applications ([Kim et al. 2020](#))
- Persistence Images ([Adams et al. 2017](#)) + Learning applications ([Som et al. 2020](#))

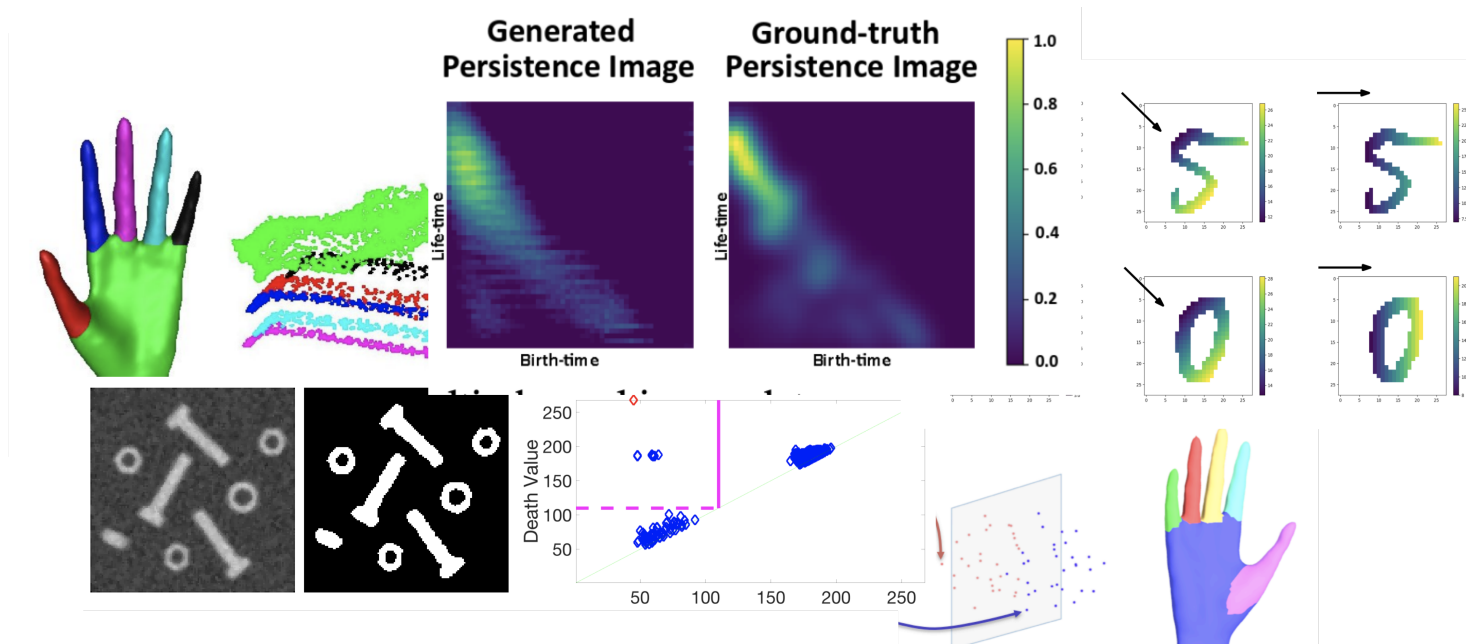


$$\rho(f, \phi) = \sum_{(i,j) \in \text{dgm}} f(i, j) \phi(|j - i|)$$

Vectorizing diagrams

There are many mappings from dgm's to function spaces (e.g. Hilbert spaces)

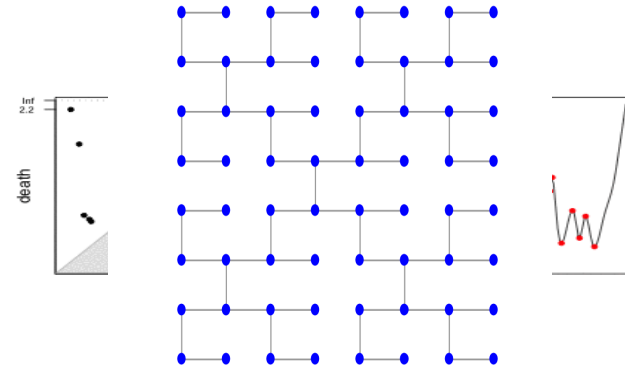
- Persistence Landscapes ([Bubenik 2020](#)) + Learning applications ([Kim et al. 2020](#))
- Persistence Images ([Adams et al. 2017](#)) + Learning applications ([Som et al. 2020](#))
- A few others...¹



See ([Bubenik 2020](#)) for an overview.

We have many goals in common...

- Vectorize persistence information
- Optimize persistence invariants
- Leverage the stability of persistence
- Connect to other areas of mathematics

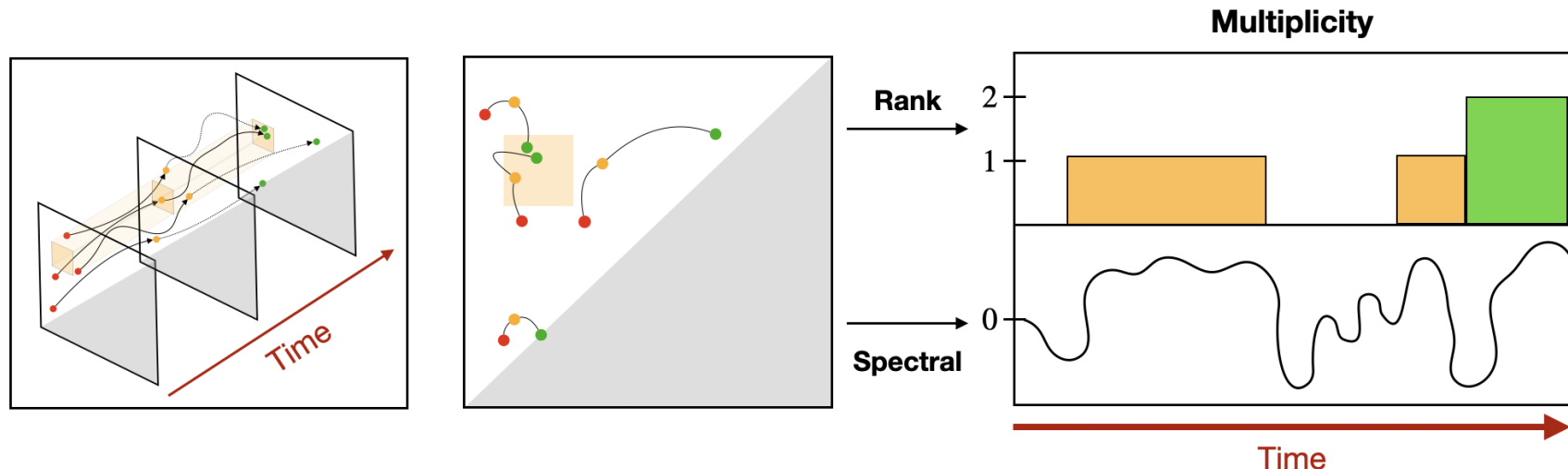


Can we achieve them without computing diagrams?*

This Talk

In this talk we introduce a *spectral-relaxation* of the rank invariant that:

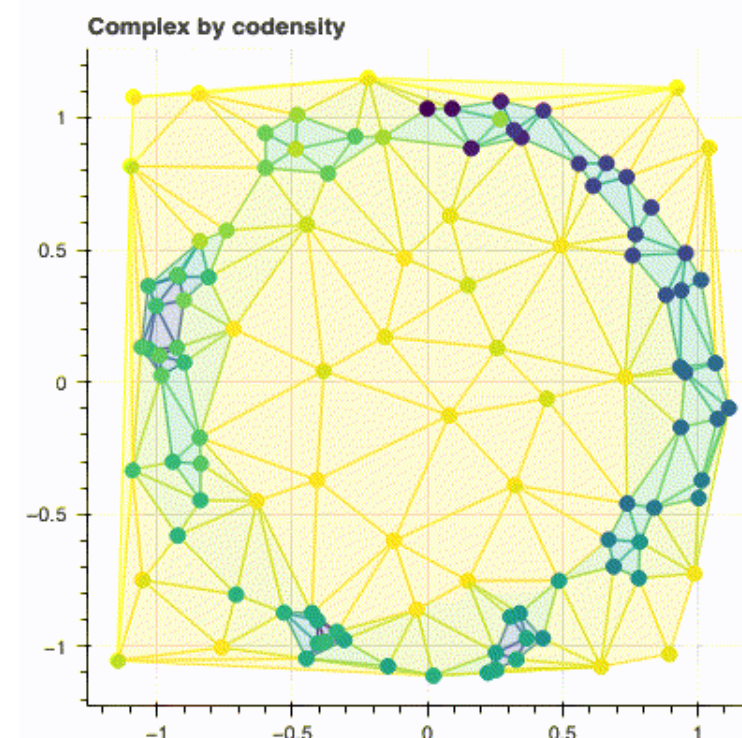
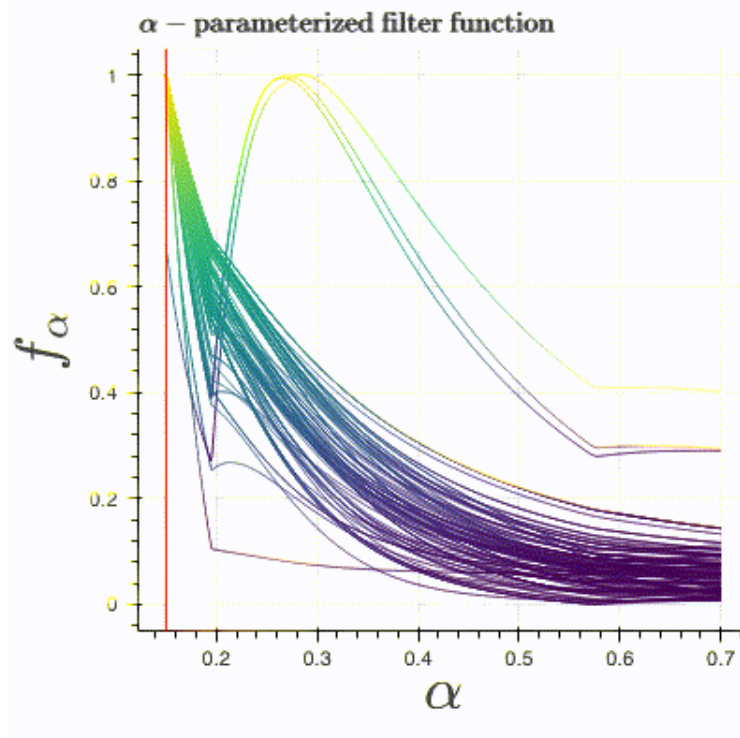
1. Continuously interpolates the *persistent rank* function
2. is smooth + differentiable on S_+
3. $(1-\epsilon)$ approximates $\beta_p^{i,j}$ for any $\epsilon > 0$ + essentially $O(n^2)$ time
4. Vectorizes non-harmonic spectra of Laplacian operators
5. Is computable in a “matrix-free” fashion in $O(n)$ memory



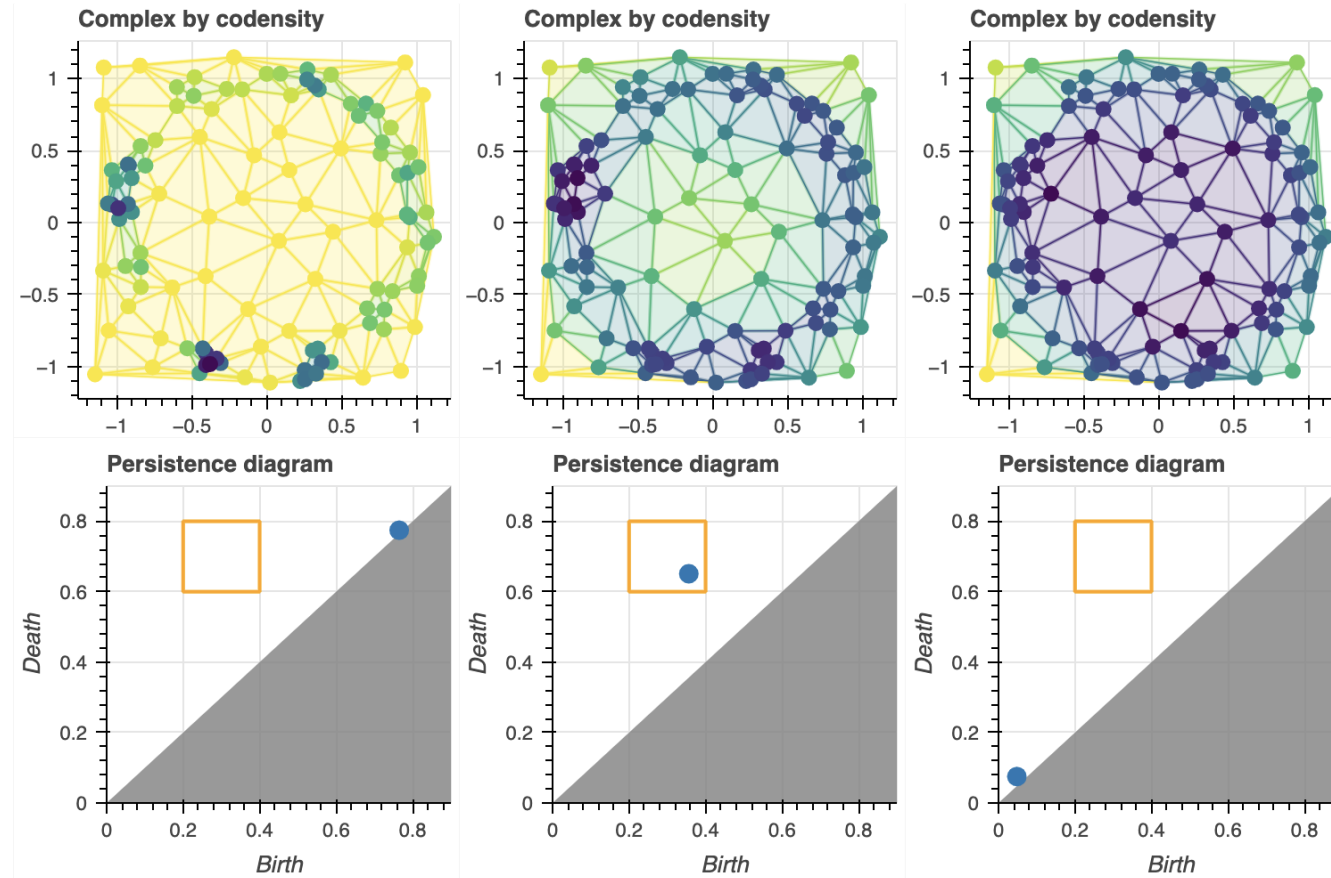
Setting: Parameterized filtrations

Suppose we have an α -parameterized filtration (K, f_α) where $f_\alpha : K \rightarrow \mathbb{R}_+$ satisfies:

$$f_\alpha(\tau) \leq f_\alpha(\sigma) \quad \text{if } \tau \subseteq \sigma \quad \forall \tau, \sigma \in K \text{ and } \alpha \in \mathbb{R}$$

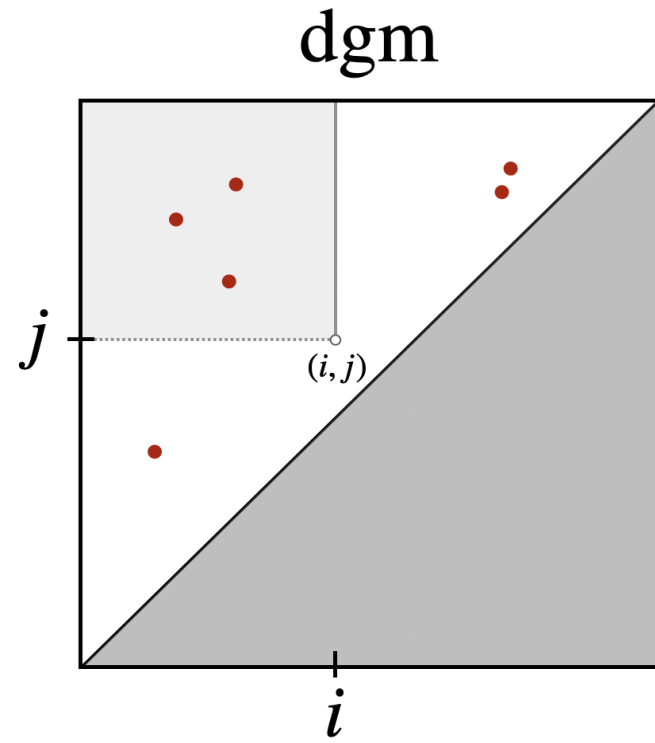


Application: optimizing filtrations

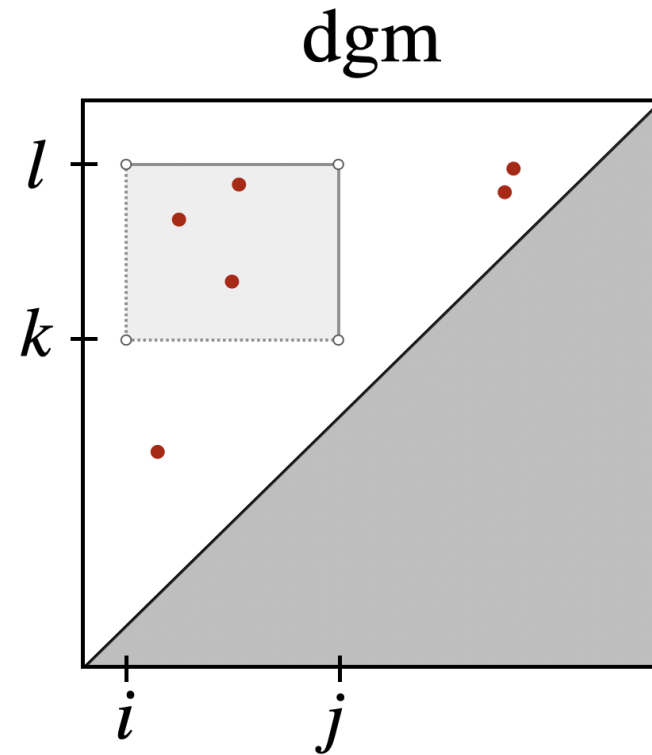


$$\alpha^* = \arg \max_{\alpha \in \mathbb{R}} \text{card}(\text{dgm}(K_\bullet, f_\alpha)|_R)$$

The rank invariants with pictures



$$\beta_p^{i,j}(K)$$



$$\mu_p^R(K)$$

Why the rank invariant?

There is a duality between diagrams its associated rank function:

$$\text{dgm}_p(K_\bullet, f) \triangleq \{ (i, j) \in \Delta_+ : \mu_p^{i,j} \neq 0 \} \cup \Delta$$

where: $\mu_p^{i,j} = (\beta_p^{i,j-1} - \beta_p^{i,j}) - (\beta_p^{i-1,j-1} - \beta_p^{i-1,j})$

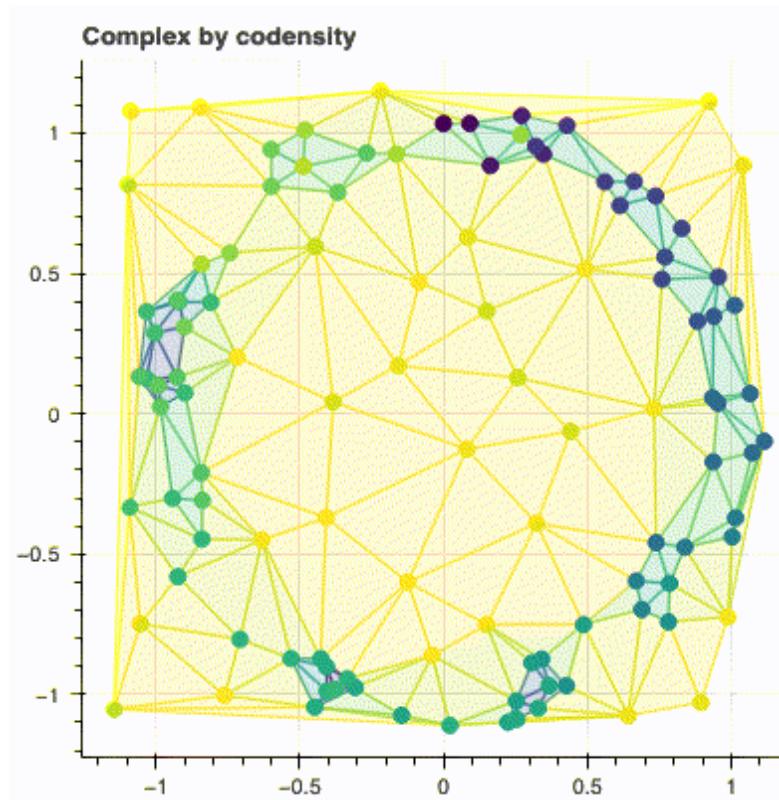
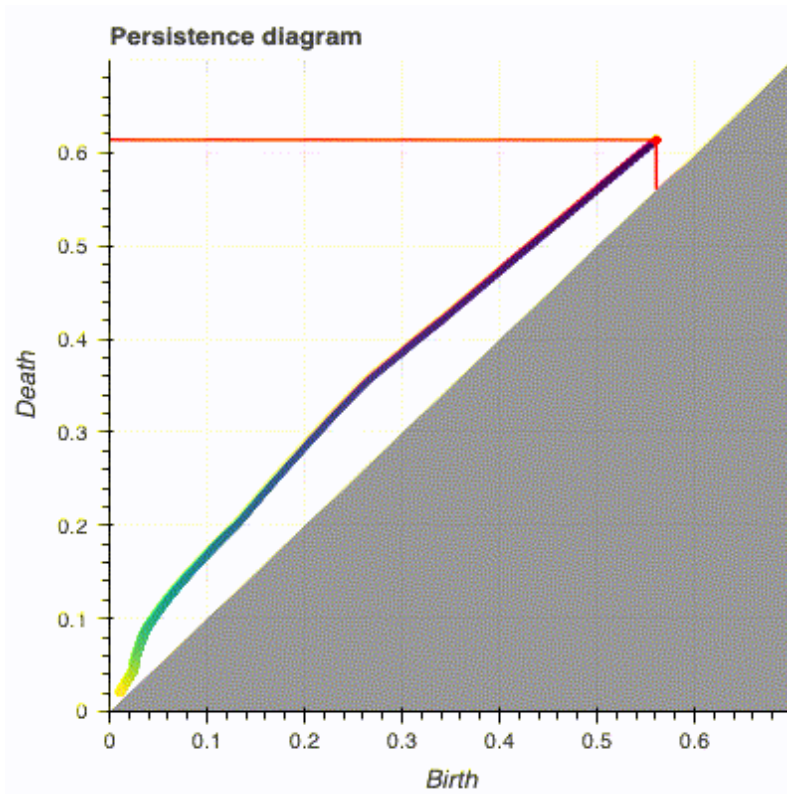
Fundamental Lemma of Persistent Homology shows diagrams characterize their ranks

$$\beta_p^{k,l} = \sum_{i \leq k} \sum_{j > l} \mu_p^{i,j}$$

- Persistence measures ([Chazal et al. 2016](#)) extend (1,2) naturally when $\mathbb{F} = \mathbb{R}$
- Stability in context of multidimensional persistence ([Cerri et al. 2013](#))
- Generalizations of rank invariant via Möbius inversion ([McCleary and Patel 2022](#)) and via zigzag persistence([Tamal K. Dey, Kim, and Mémoli 2021](#))

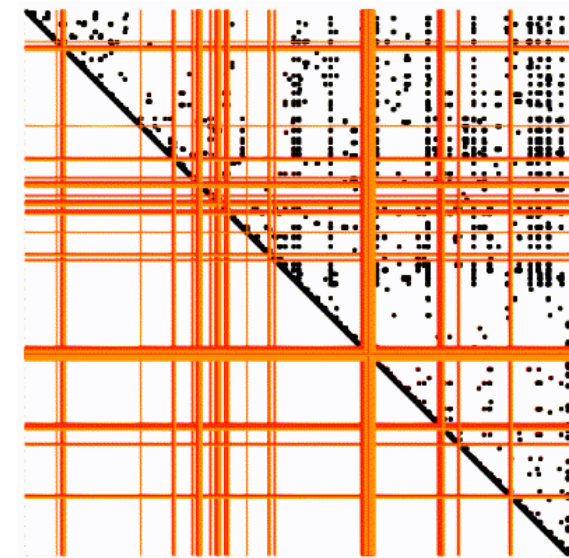
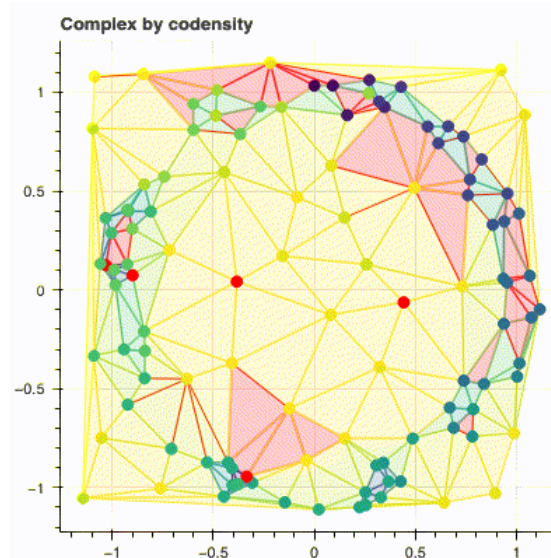
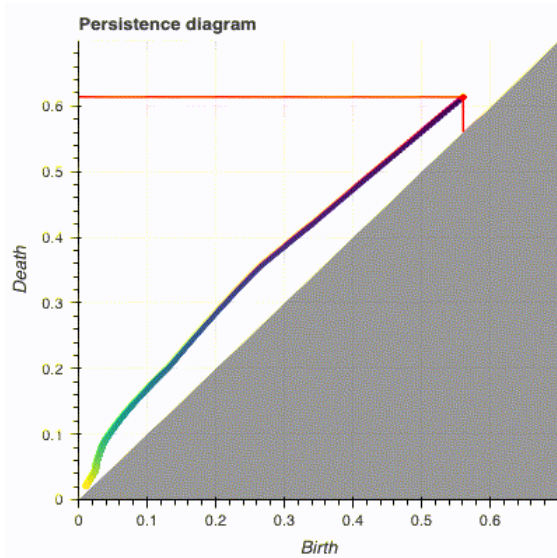
Why not use diagrams?

Pro: Diagrams are stable, well-studied, and information rich.



Why not use diagrams?

Con: Extending the $R = \partial V$ to parameterized settings is highly non-trivial



Maintaining the $R = \partial V$ decomposition “across time” \implies huge memory bottleneck

For more details on the computations, see “Move Schedules” Piekenbrock and Perea (2021)

Revisiting the rank computation

$$\beta_p^{i,j} : \text{rank}(H_p(K_i) \rightarrow H_p(K_j))$$

$$\begin{aligned}\beta_p^{i,j} &= \dim\left(\text{Ker}(\partial_p(K_i)) / \text{Im}(\partial_{p+1}(K_j))\right) \\ &= \dim\left(\text{Ker}(\partial_p(K_i)) / (\text{Ker}(\partial_p(K_i)) \cap \text{Im}(\partial_{p+1}(K_j)))\right) \\ &= \text{dim}(\text{Ker}(\partial_p(K_i))) - \text{dim}(\text{Ker}(\partial_p(K_i)) \cap \text{Im}(\partial_{p+1}(K_j)))\end{aligned}$$

Rank-nullity yields the **left term**:

$$\dim(\text{Ker}(\partial_p(K_i))) = |C_p(K_i)| - \dim(\text{Im}(\partial_p(K_i)))$$

Computing the **right term** more nuanced:

- Pseudo-inverse¹, projectors², Neumann's inequality³, etc.
- PID algorithm⁴, Reduction algorithm⁵, Persistent Laplacian⁶

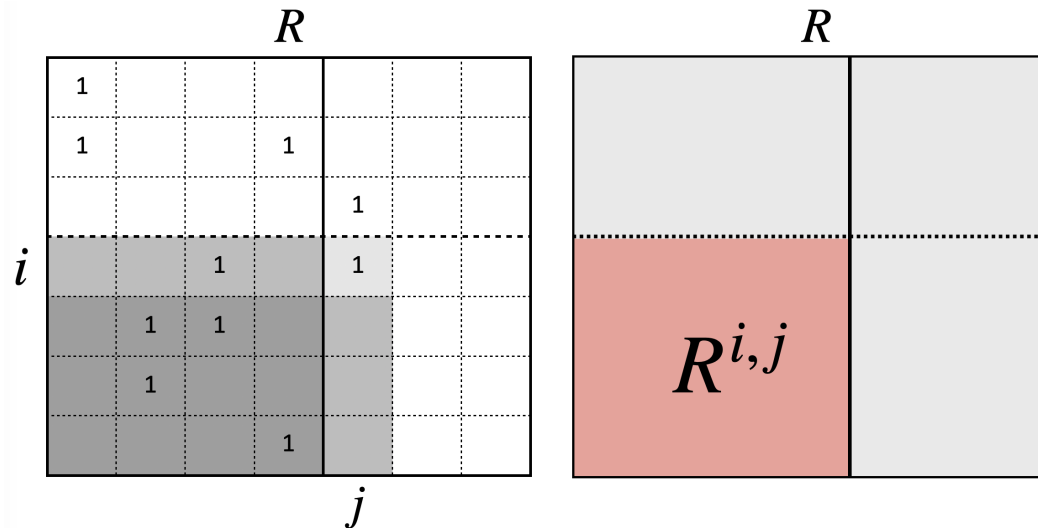
Anderson Jr and Duffin (1969), Ben-Israel (1967), Ben-Israel (2015), Zomorodian and Carlsson (2004), Edelsbrunner, Letscher, and Zomorodian (2000), Mémoli, Wan, and Wang (2022)

Key technical observation

Structure theorem for persistence modules can be used to show:

$$(i, j) \in \text{dgm}(K_\bullet)$$

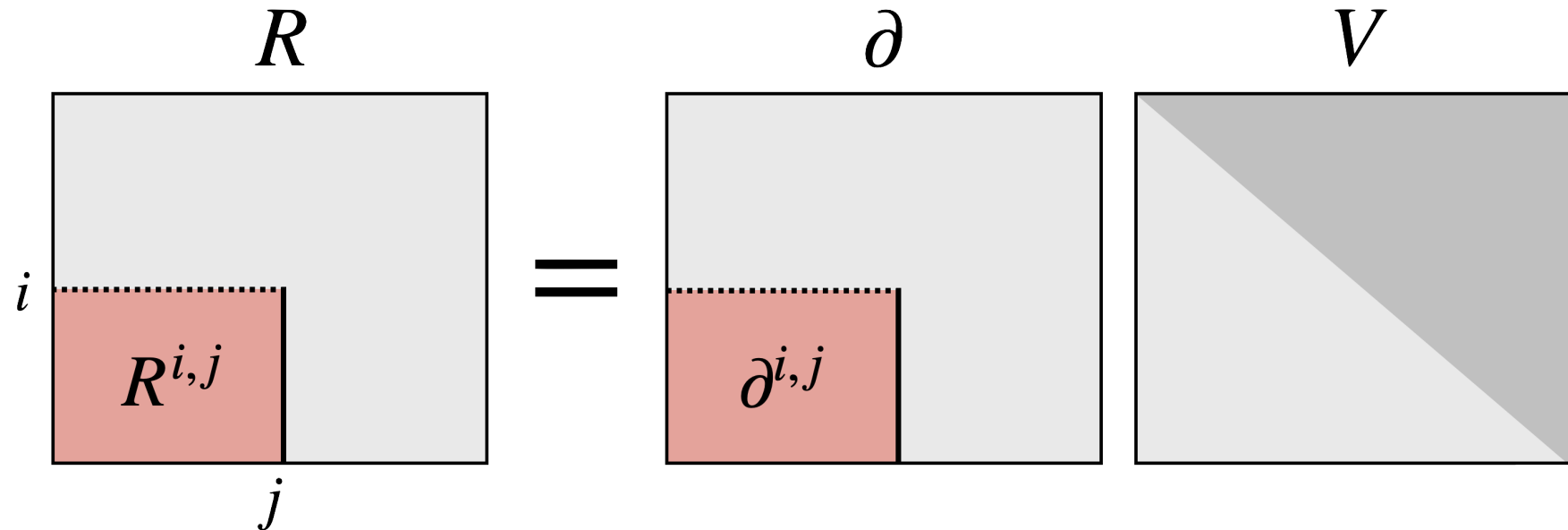
$$\Leftrightarrow \text{rank}(R^{i,j}) - \text{rank}(R^{i+1,j}) + \text{rank}(R^{i+1,j-1}) - \text{rank}(R^{i,j-1}) \neq 0$$



$$\Rightarrow \text{rank}(R^{i,j}) = \text{rank}(\partial^{i,j})$$

Key technical observation

$$\text{rank}(R^{i,j}) = \text{rank}(\partial^{i,j})$$



Take-a-way: Can deduce the dgm from ranks of “lower-left” submatrices of $\partial_p(K_\bullet)$

Key technical observation

$$\text{rank}(R^{i,j}) = \text{rank}(\partial^{i,j}) \quad (1)$$

(1) often used to show correctness of reduction, but far more general, as it implies:

Corollary (Bauer et al. 2022): Any algorithm that preserves the ranks of the submatrices $\partial^{i,j}$ for all $i, j \in \{1, \dots, n\}$ is a valid barcode algorithm.

$$(1) \Rightarrow \beta_p^{i,j} = |C_p(K_i)| - \text{rank}(\partial_p^{1,i}) - \text{rank}(\partial_{p+1}^{1,j}) + \text{rank}(\partial_{p+1}^{i+1,j}) \quad (2)$$

$$(2) \Rightarrow \mu_p^R = \text{rank}(\partial_{p+1}^{j+1,k}) - \text{rank}(\partial_{p+1}^{i+1,k}) - \text{rank}(\partial_{p+1}^{j+1,l}) + \text{rank}(\partial_{p+1}^{i+1,l}) \quad (3)$$

Edelsbrunner, Letscher, and Zomorodian (2000) noted (1) in passing showing correctness of reduction; Tamal Krishna Dey and Wang (2022) explicitly prove (2); (3) was used by Chen and Kerber (2011). (2) & (3) are connected to relative homology.

Overview

- Introduction & Motivation
 - Diagram vectorization and optimization
 - The effective intractability of reduction
 - Duality between diagrams and their ranks
- Derivation of relaxation
 - Parameterizing p -chains with \mathbb{R} coefficients
 - Replacing boundary operators with Löwner operators
 - Connections to combinational Laplacians
- Experiments
 - Shape signatures via directional transform
 - Shape signatures via intrinsic metrics
 - Codensity example

The Implication: Rank Invariance

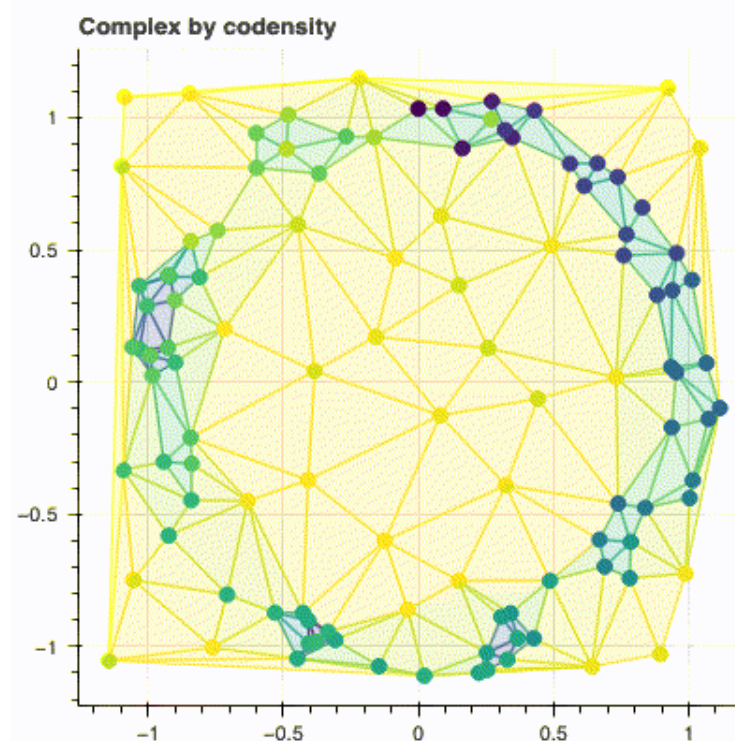
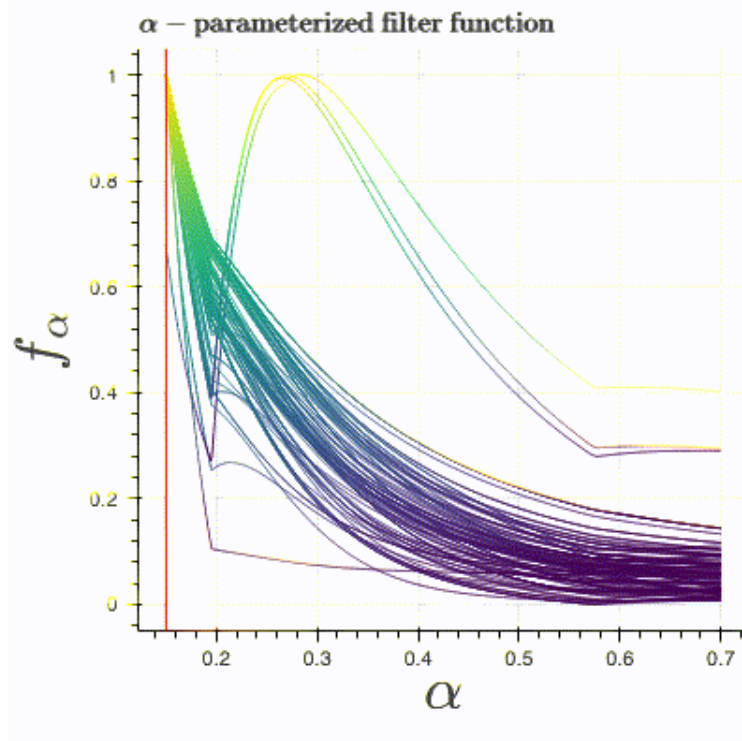
$$\begin{aligned}\text{rank}(A) &\triangleq \dim(\text{Im}(A)) \\ &\equiv \text{rank}(A^T) && (\text{adjoint}) \\ &\equiv \text{rank}(A^T A) && (\text{inner product}) \\ &\equiv \text{rank}(A A^T) && (\text{outer product}) \\ &\equiv \text{rank}(S^{-1} A S) && (\text{change of basis}) \\ &\equiv \text{rank}(P^T A P) && (\text{permutation}) \\ &\equiv \dots && (\text{many others})\end{aligned}$$

Q: Can we exploit some of these to speed up the computation?

Parameterized filtrations

Suppose we have an α -parameterized filtration (K, f_α) where $f_\alpha : K \rightarrow \mathbb{R}_+$ satisfies:

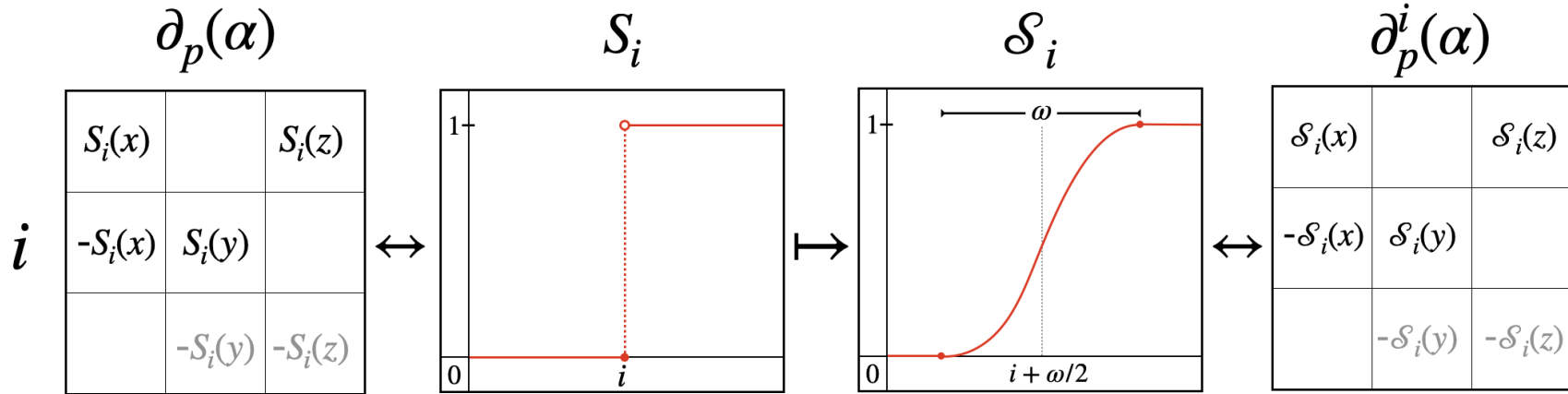
$$f_\alpha(\tau) \leq f_\alpha(\sigma) \quad \text{if } \tau \subseteq \sigma \quad \forall \tau, \sigma \in K$$



Parameterized *boundary matrices*

Idea #1: Parameterize p -chains $c \in C_p(K; \mathbb{R})$ with $f_\alpha : K \rightarrow \mathbb{R}_+$

$$\partial_p^{i,j}(\alpha) = D_p(\mathcal{S}_i \circ f_\alpha) \circ \partial_p(K) \circ D_{p+1}(\mathcal{S}_j \circ f_\alpha)$$



Replacing $S \mapsto \mathcal{S}$ ensures $\partial_p^{i,j}(\alpha)$ is element-wise continuous

Note: $\partial_p^{i,j}(\alpha)$ has rank = $\text{rank}(R_p^{i,j}(\alpha))$ for all $\alpha \in \mathbb{R}$.

Spectral functions

Idea #2: Approximate rank with *spectral functions* (Bhatia 2013)

$$\begin{aligned} \text{rank}(X) &= \|\sigma\|_0 && \text{where } X = U \text{Diag}(\sigma) V^T \\ &= \sum_{i=1}^n \text{sgn}_+(\sigma_i) && \text{where } \text{sgn}_+(x) \triangleq \mathbf{1}(x > 0) \\ &\approx \sum_{i=1}^n \phi(\sigma_i, \epsilon) && \text{where } \phi(x, \epsilon) \triangleq \int_{-\infty}^x \hat{\delta}(z, \epsilon) dz \\ &= \|\Phi_\epsilon(X)\|_* && \text{where } \Phi_\epsilon(X) \triangleq \sum_{i=1}^n \phi(\sigma_i, \epsilon) u_i v_i^T \end{aligned}$$

$\Phi_\epsilon(X)$ is a Löwner operator when ϕ is operator monotone (Jiang and Sendov 2018)

$$A \succeq B \implies \Phi_\epsilon(A) \succeq \Phi_\epsilon(B)$$

Used in convex analysis + nonexpansive mappings (Bauschke, Combettes, et al. 2011)

Lowner Operators

(Bi, Han, and Pan 2013) show that for any smoothed Dirac delta function¹ $\hat{\delta}$ and differentiable *operator monotone* function $\phi : \mathbb{R}_+ \times \mathbb{R}_{++} \rightarrow \mathbb{R}_+$, we have:

(ϵ -close)	$0 \leq \text{rank}(X) - \ \Phi_\epsilon(X)\ _* \leq c(\hat{\delta})$
(Monotonicity)	$\ \Phi_\epsilon(X)\ _* \geq \ \Phi_{\epsilon'}(X)\ _*$ for any $\epsilon \leq \epsilon'$
(Smooth)	Lipshitz + semismooth ² on $\mathbb{R}^{n \times m}$
(Computable)	Closed-form soln. to differential $\partial \ \Phi_\epsilon(\cdot)\ _*$
(Differentiable)	Continuously differentiable on \mathbf{S}_+^m

Small issue: $\partial_p^*(\alpha) \in \mathbb{R}^{n \times m}$ (not in \mathbf{S}_+^m)

Easy fix: $\Phi_\epsilon(\partial_p \circ \partial_p^T)(\alpha)$ or $\Phi_\epsilon(\partial_p^T \circ \partial_p)(\alpha)$

1. Any $\hat{\delta}$ of the form $\nu(1/\epsilon)p(z \cdot \nu(1/\epsilon))$ where p is a density function and ν positive and increasing is sufficient.
2. Here *semismooth* refers the existence of directional derivatives

Combinatorial Laplacian

3rd idea: parameterize using *combinatorial Laplacians* ([Horak and Jost 2013](#)):

$$\Delta_p = \underbrace{\partial_{p+1} \partial_{p+1}^T}_{L_p^{\text{up}}} + \underbrace{\partial_p^T \partial_p}_{L_p^{\text{dn}}}$$

f_α is 1-to-1 correspondence with inner products on cochain groups $C^p(K, \mathbb{R})$

$$L_p^{i,j}(\alpha) \Leftrightarrow \langle f, g \rangle_\alpha \text{ on } C^{p+1}(K)$$

Have “nice” linear and quadratic forms, e.g.:

$$L_p^{\text{up}}(\tau, \tau') = \begin{cases} \deg_f(\tau) \cdot f^{+/2}(\tau) & \text{if } \tau = \tau' \\ s_{\tau, \tau'} \cdot f^{+/2}(\tau) \cdot f(\sigma) \cdot f^{+/2}(\tau') & \text{if } \tau \stackrel{\sigma}{\sim} \tau' \\ 0 & \text{otherwise} \end{cases}$$

⇒ can represent operator in “matrix-free” fashion

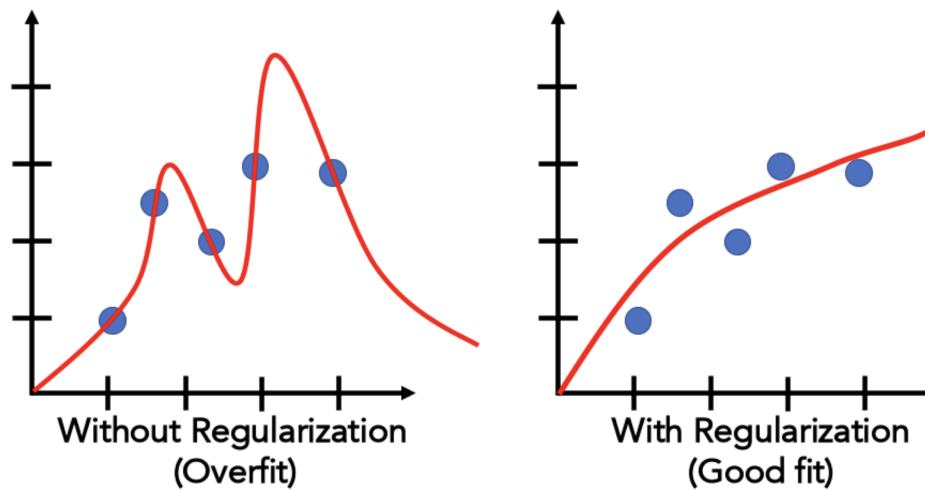
Regularization interpretation

Instead of solving $Ax = b$, consider the “regularized” least-squares objective:

$$x_\epsilon^* = \arg \min_{x \in \mathbb{R}^n} \|Ax - b\|^2 + \epsilon \|x\|_1$$

The minimizer is given in closed-form by the regularized pseudo-inverse:

$$x_\epsilon^* = (A^T A + \epsilon I)^{-1} A^T b$$



Regularization interpretation

$$x_\epsilon^* = \arg \min_{x \in \mathbb{R}^n} \|Ax - b\|^2 + \epsilon \|x\|^2 = (A^T A + \epsilon I)^{-1} A^T b$$

Under the appropriate hyper-parameter settings¹, ϕ takes the form:

$$\phi(x, \epsilon) = \int_{-\infty}^x \hat{\delta}(z, \epsilon) dz = \frac{x^2}{x^2 + \epsilon}$$

The corresponding Lowner operator and its Schatten 1-norm is given by:

$$\Phi_\epsilon(X) = (X^T X + \epsilon I_n)^{-1} X^T X, \quad \|\Phi_\epsilon(X)\|_* = \sum_{i=1}^n \frac{\sigma_i(X)^2}{\sigma_i(X)^2 + \epsilon}$$

This the *Tikhonov regularization* in standard form used in ℓ_1 -regression (LASSO)

1. This ϕ corresponds to setting $\nu(\epsilon) = \sqrt{\epsilon}$ and $p(x) = 2x(x^2 + 1)^{-2}$.

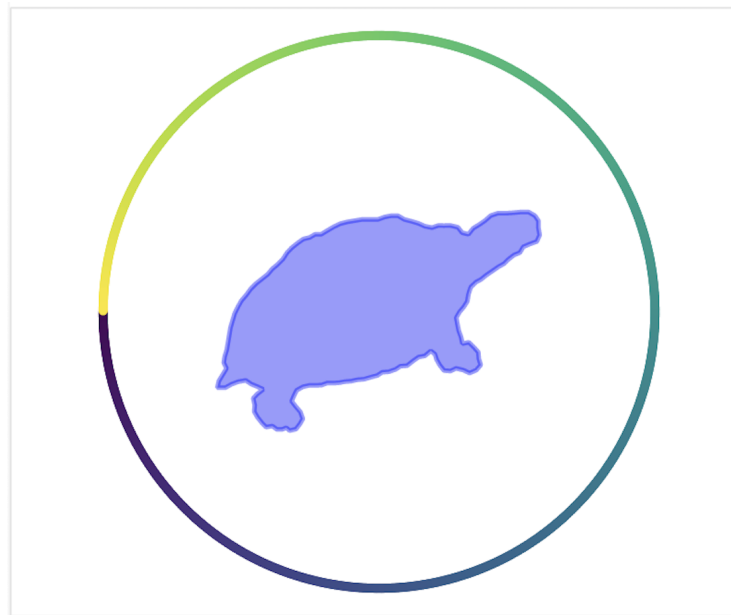
Overview

- Introduction & Motivation
 - Diagram vectorization and optimization
 - The effective intractability of reduction
 - Duality between diagrams and their ranks
- Derivation of relaxation
 - Parameterizing p -chains with \mathbb{R} coefficients
 - Replacing boundary operators with Löwner operators
 - Connections to combinational Laplacians
- Experiments
 - Shape signatures via directional transform
 - Shape signatures via intrinsic metrics
 - Codensity example

Experiment #1: Directional Transform

Consider “looking” at a complex K embedded in R^d

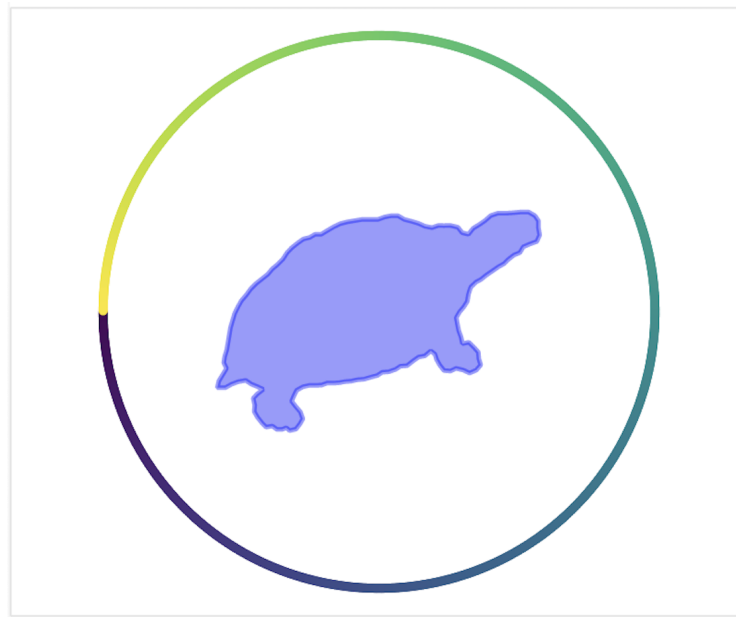
$$\begin{aligned}\text{DT}(K) : S^{d-1} &\rightarrow K \times C(K, \mathbb{R}) \\ v &\mapsto (K_\bullet, f_v)\end{aligned}$$



$$K_\bullet = K(v)_i = \{ x \in X \mid \langle x, v \rangle \leq i \}$$

Experiment #1: Directional Transform

$$K_{\bullet} = K(v)_i = \{ x \in X \mid \langle x, v \rangle \leq i \}$$



$$\{ \text{dgm}(v) : v \in S^{d-1} \} \Leftrightarrow \text{PHT}$$

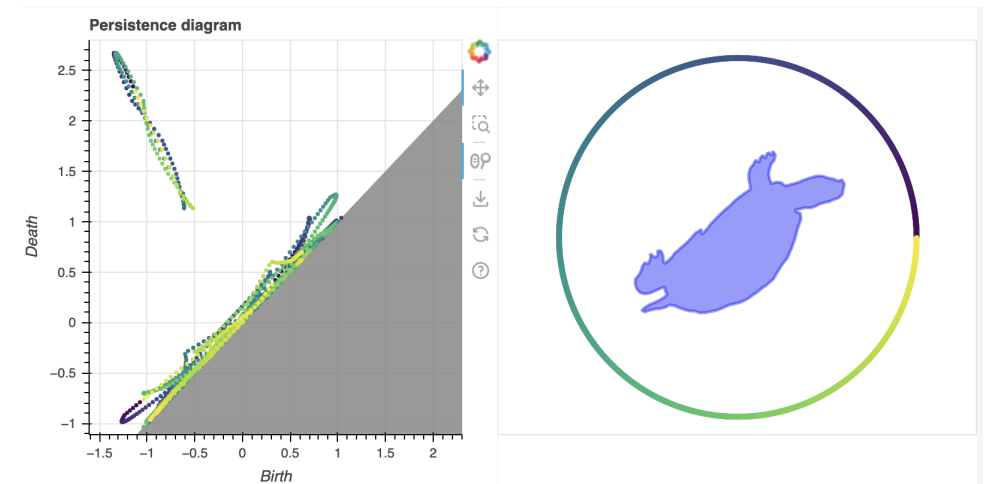
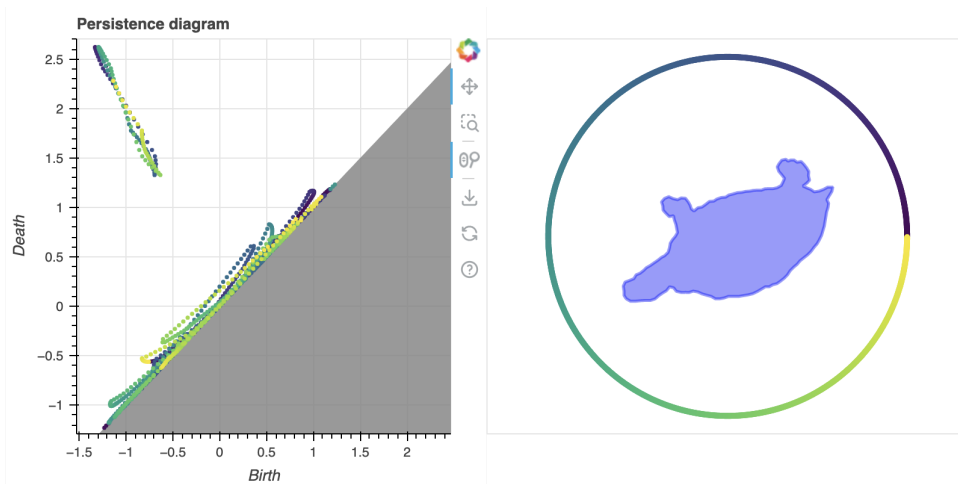
$$\{ \chi(v) : v \in S^{d-1} \} \Leftrightarrow \text{ECT}$$

Experiment #1: Directional Transform

$$K_{\bullet} = K(v)_i = \{ x \in X \mid \langle x, v \rangle \leq i \}$$

Injectivity of the PHT \leftrightarrow endow a metric \mathcal{D} by integrating d_B (or d_W) over S_{d-1}

$$d_{\text{PHT}}(\text{dgm}_X, \text{dgm}_Y) := \sum_{p=0}^d \int_{S^{d-1}} d_B(\text{dgm}(X, v)), (\text{dgm}(Y, v)) dv$$

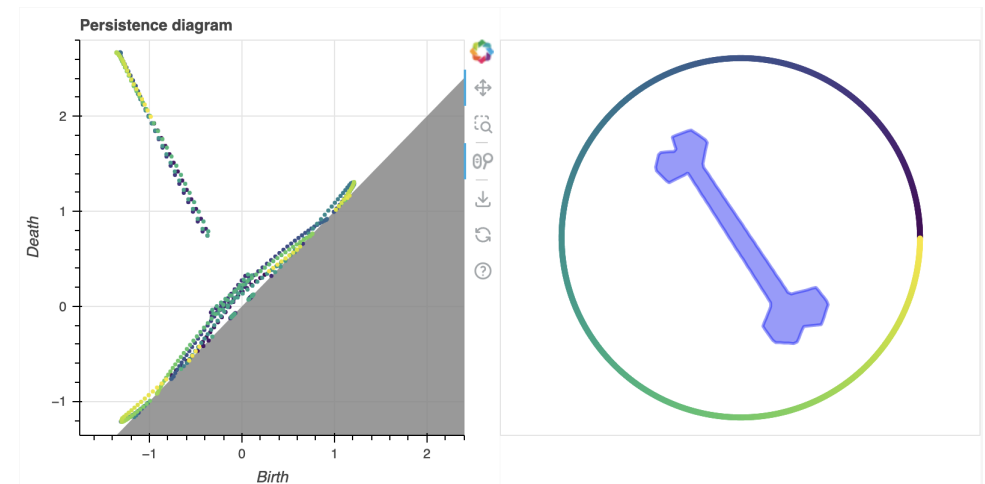
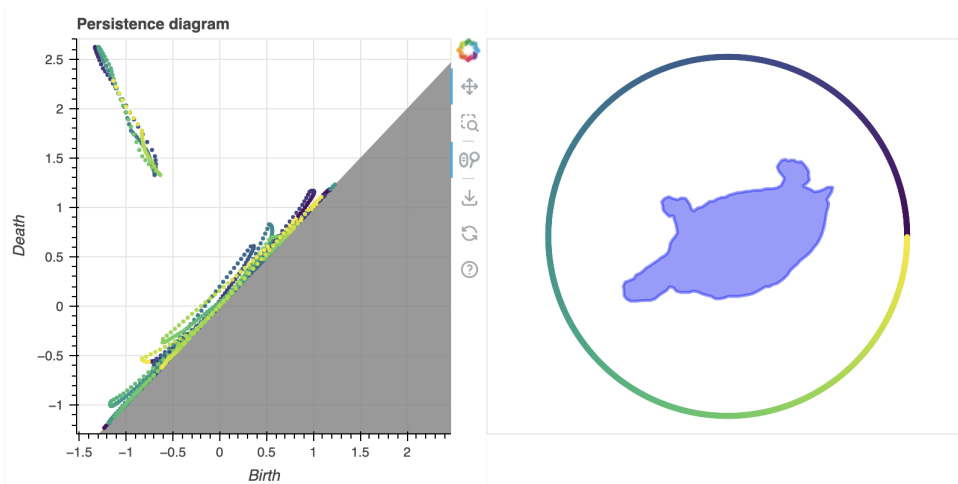


Experiment #1: Directional Transform

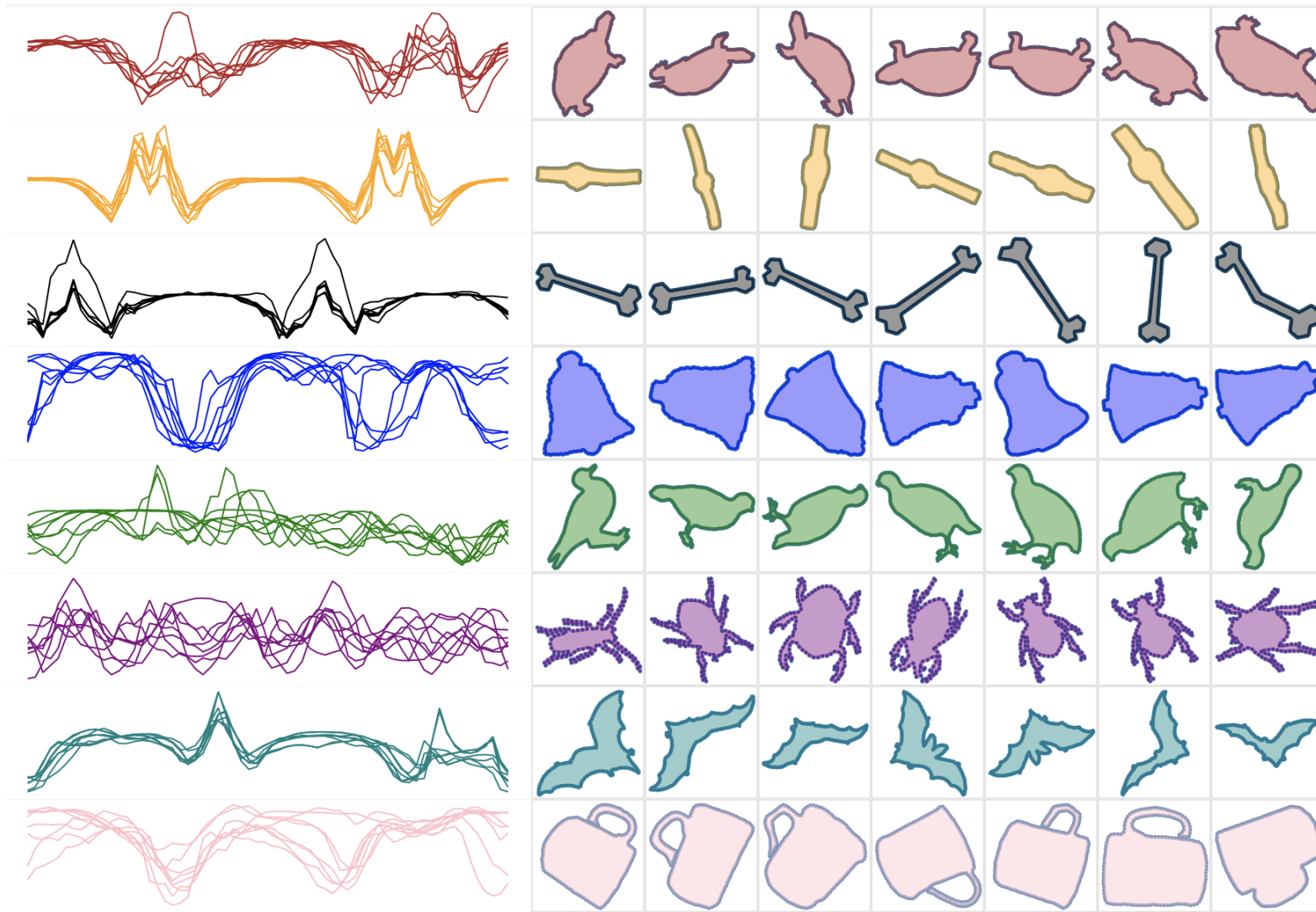
$$K_\bullet = K(v)_i = \{ x \in X \mid \langle x, v \rangle \leq i \}$$

Injectivity of the PHT \leftrightarrow endow a metric \mathcal{D} by integrating d_B (or d_W) over S_{d-1}

$$d_{\text{PHT}}(\text{dgm}_X, \text{dgm}_Y) := \sum_{p=0}^d \int_{S^{d-1}} d_B(\text{dgm}(X, v)), (\text{dgm}(X, v)) dv$$

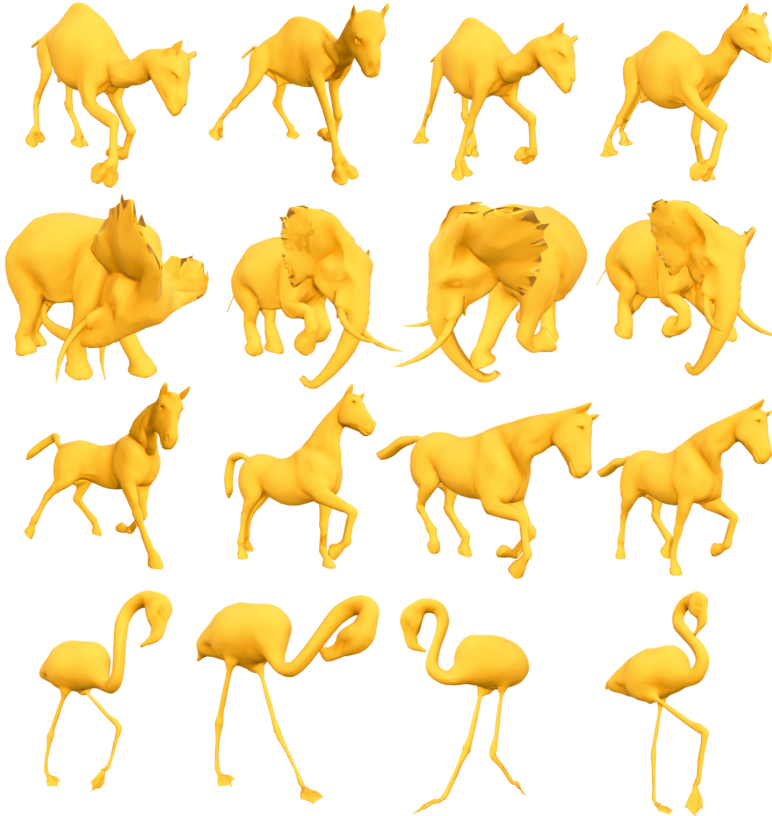


Experiment #1: Directional Transform



Experiment #2: Intrinsic signatures

Dataset: 3D meshes of animals in different poses ([Chazal et al. 2009](#))

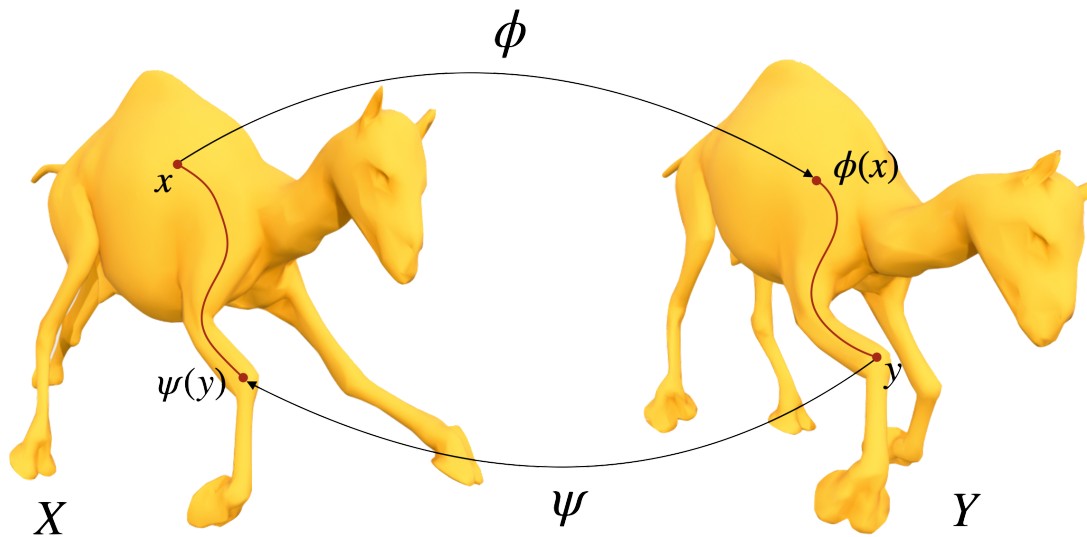


Challenge: Recognize intrinsic shape categories (via a distance metric)

Experiment #2: Intrinsic signatures

The Gromov-Hausdorff distance yields a metric on the set of compact metric spaces \mathcal{X}

$$d_{GH}(d_X, d_Y) = \sup_{x \in X, y \in Y} |d_X(x, \psi(y)) - d_Y(\phi(x), y)|$$



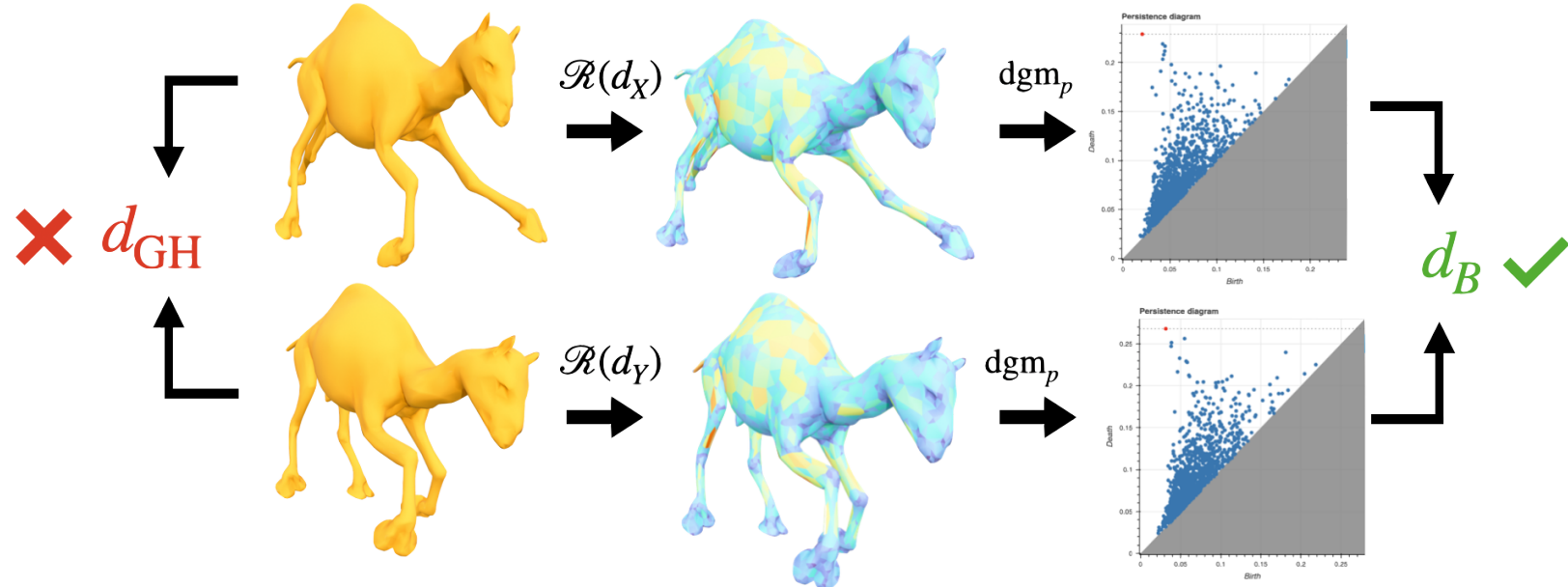
Using intrinsic metric makes d_{GH} blind to e.g. shapes represented in different *poses*

Unfortunately, the GH distance is NP-hard to compute ([Mémoli 2012](#))

Experiment #2: Intrinsic signatures

It's known d_B (d_W) on Rips filtrations $\mathcal{R}(X, d_X)$ lower bound GH (GW) distance

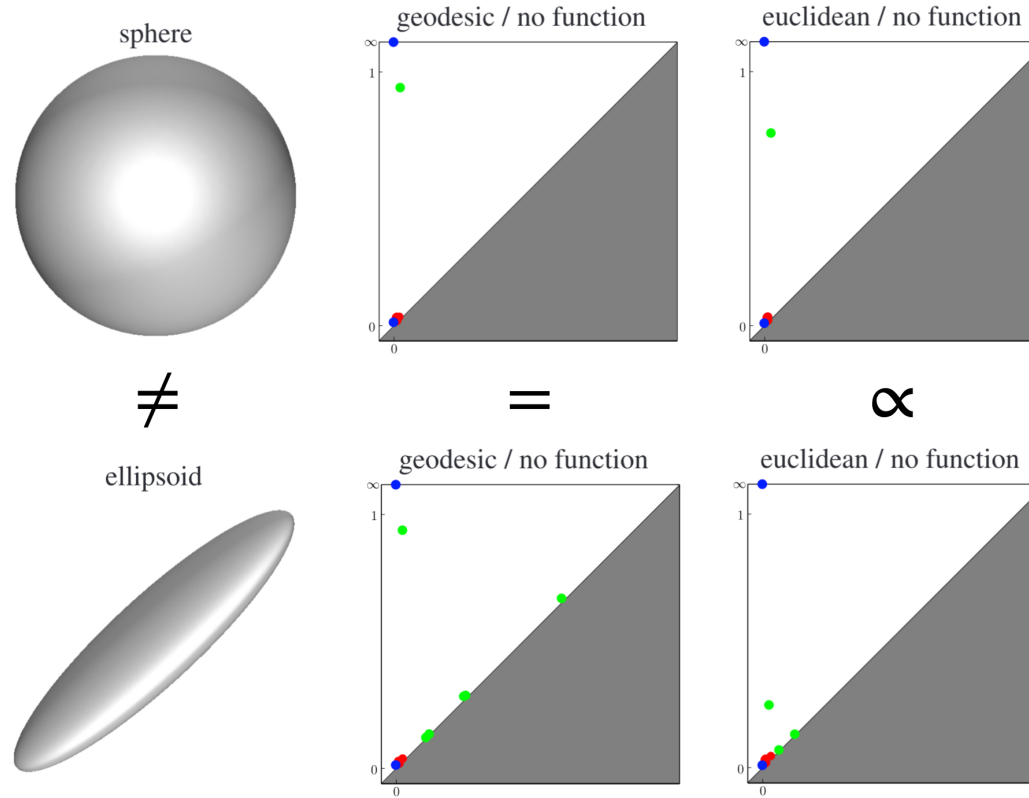
$$d_B(\mathrm{dgm}_p(\mathcal{R}(X, d_X)), \mathrm{dgm}_p(\mathcal{R}(Y, d_Y))) \leq d_{GH}((X, d_X), (Y, d_Y))$$



Motivates use of persistence in metric settings for e.g. shape classification!

Experiment #2: Intrinsic signatures

Issue: Diagrams are far from injective, cannot distinguish e.g. stretched shapes



The lower bound on d_{GH} could be totally useless!

Experiment #2: Intrinsic signatures

Lower bounds extend to Rips filtrations *augmented* with real-valued functions f, g :

$$\mathcal{R}(f) \triangleq \mathcal{R}(X, d_X, f) = \{\mathcal{R}_\alpha(X_\alpha)\}_{\alpha>0}, \quad X_\alpha \triangleq f^{-1}((-\infty, \alpha)) \subseteq X$$

The diagrams from $\mathcal{R}(\lambda \cdot f_X)$ represent *stable signatures* for each $\lambda > 0$:

$$d_B(\mathcal{R}(\lambda \cdot f_X), \mathcal{R}(\lambda \cdot f_Y)) \leq \max(1, \lambda L) \cdot d_{\text{GH}}(X, Y)$$

Chazal showed these bounds extend to metrics on *augmented* metric spaces:

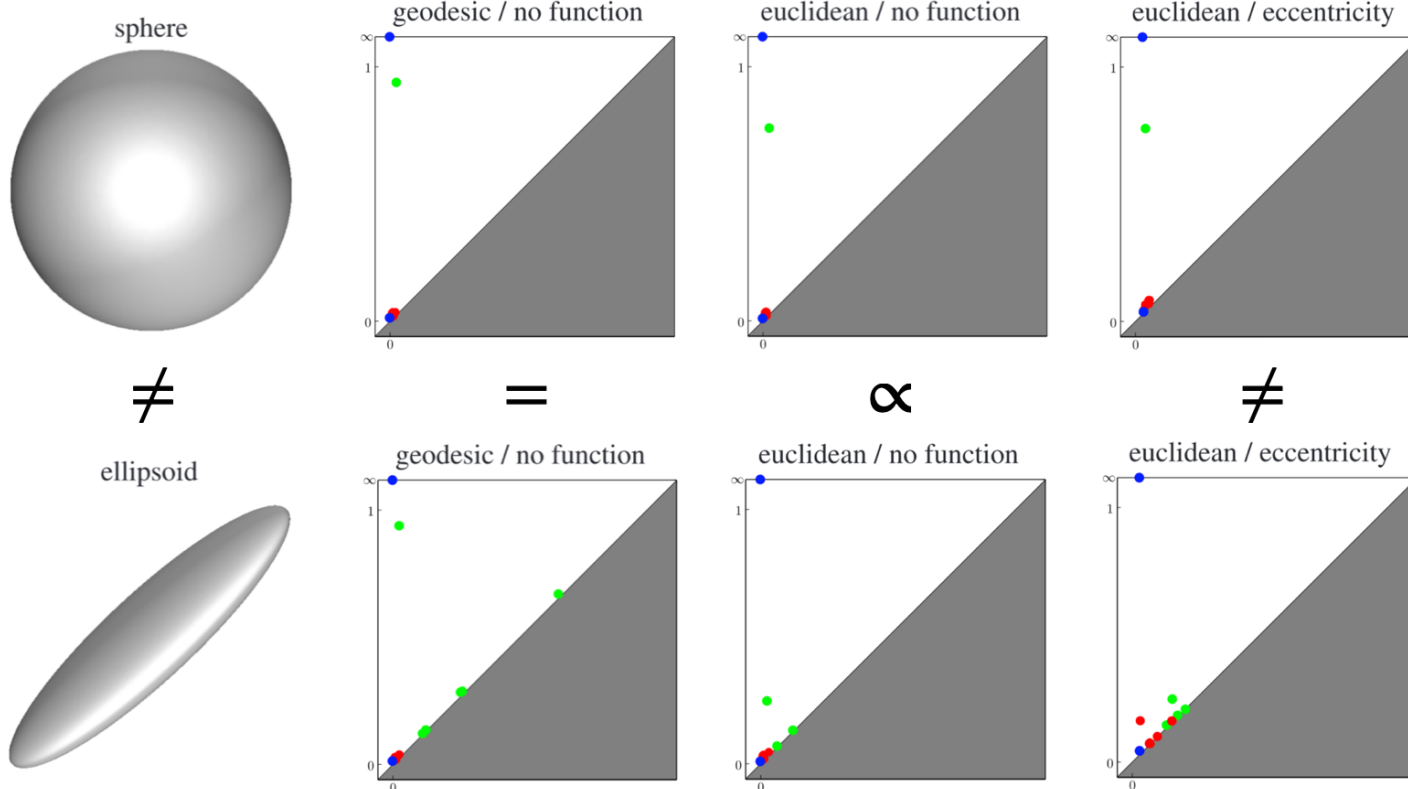
$$\mathcal{X}_1 = \{(X, d_X, f_X) \mid (X, d_X, f_X) \in \mathcal{X}, f_X : X \rightarrow \mathbb{R} \text{ continuous}\}$$

These signatures also extend to measure metric spaces, see ([Chazal et al. 2009](#))

NOTE: Size of L depends on the choice of f + each λ produces a new signature!

Experiment #2: Intrinsic signatures

Ex: The eccentricity function $e_X^1(x) = \max_{x' \in X} d_X(x, x')$ has $L = 2$

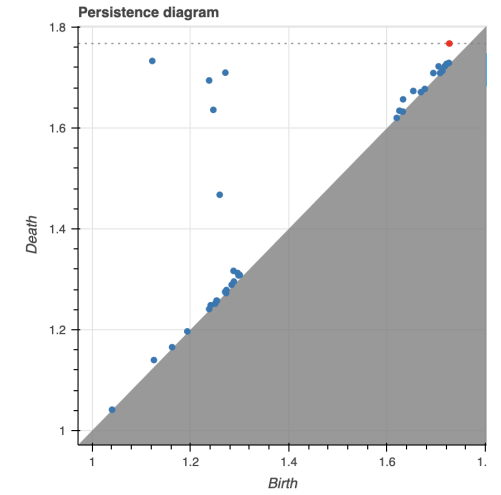
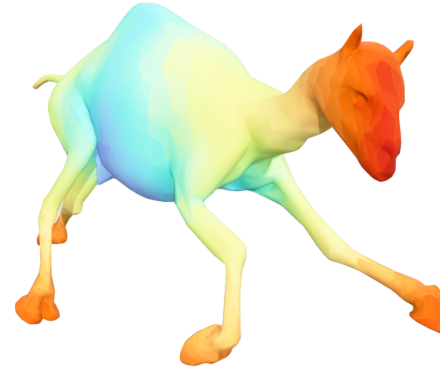
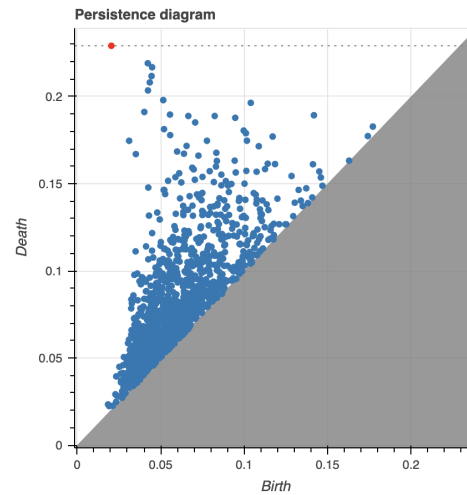
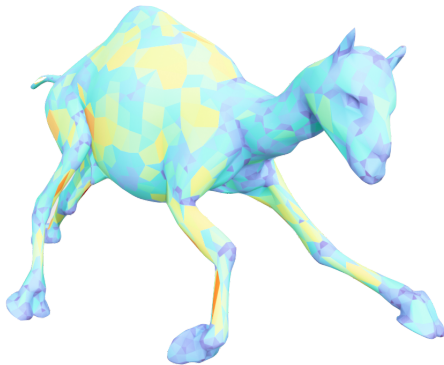


Augmenting via a fraction of e_X^1 modifies the diagrams of the ellipsoid significantly

Experiment #2: Intrinsic signatures

Lower bounds extend to Rips filtrations *augmented* with real-valued functions f, g :

$$d_B(\mathcal{R}(\lambda \cdot f_X), \mathcal{R}(\lambda \cdot f_Y)) \leq \max(1, \lambda L) \cdot d_{\text{GH}}(X, Y)$$

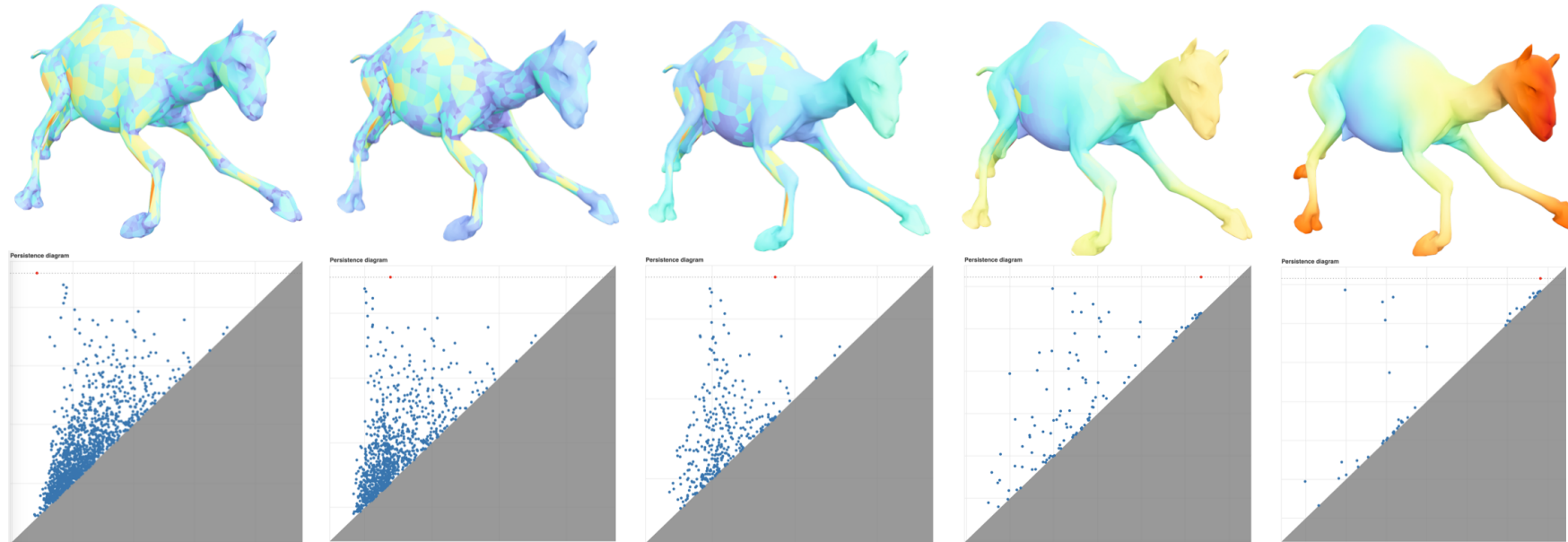


Larger values of λ yield worse bounds, but can lead to simpler diagrams

Experiment #2: Intrinsic signatures

Each choice of $\lambda > 0$ yields a *stable signature* via $\mathcal{R}(\lambda \cdot f_X)$

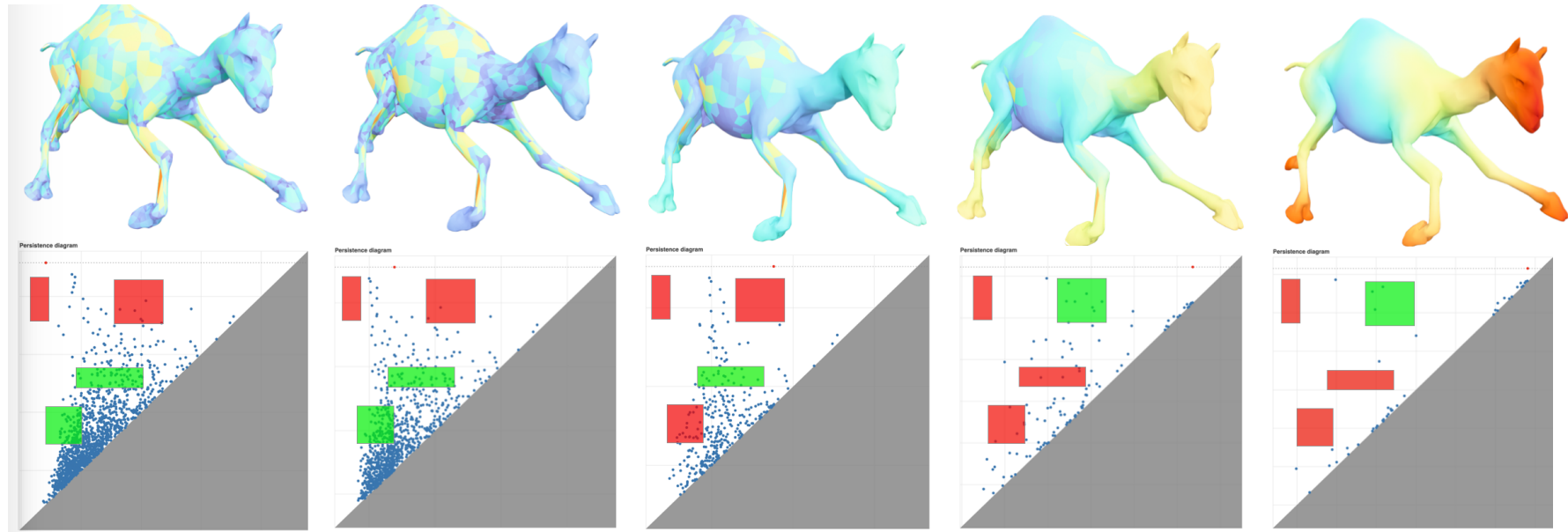
Which value of λ to choose?



Experiment #2: Intrinsic signatures

Each choice of $\lambda > 0$ yields a *stable signature* via $\mathcal{R}(\lambda \cdot f_X)$

Which value of λ to choose?

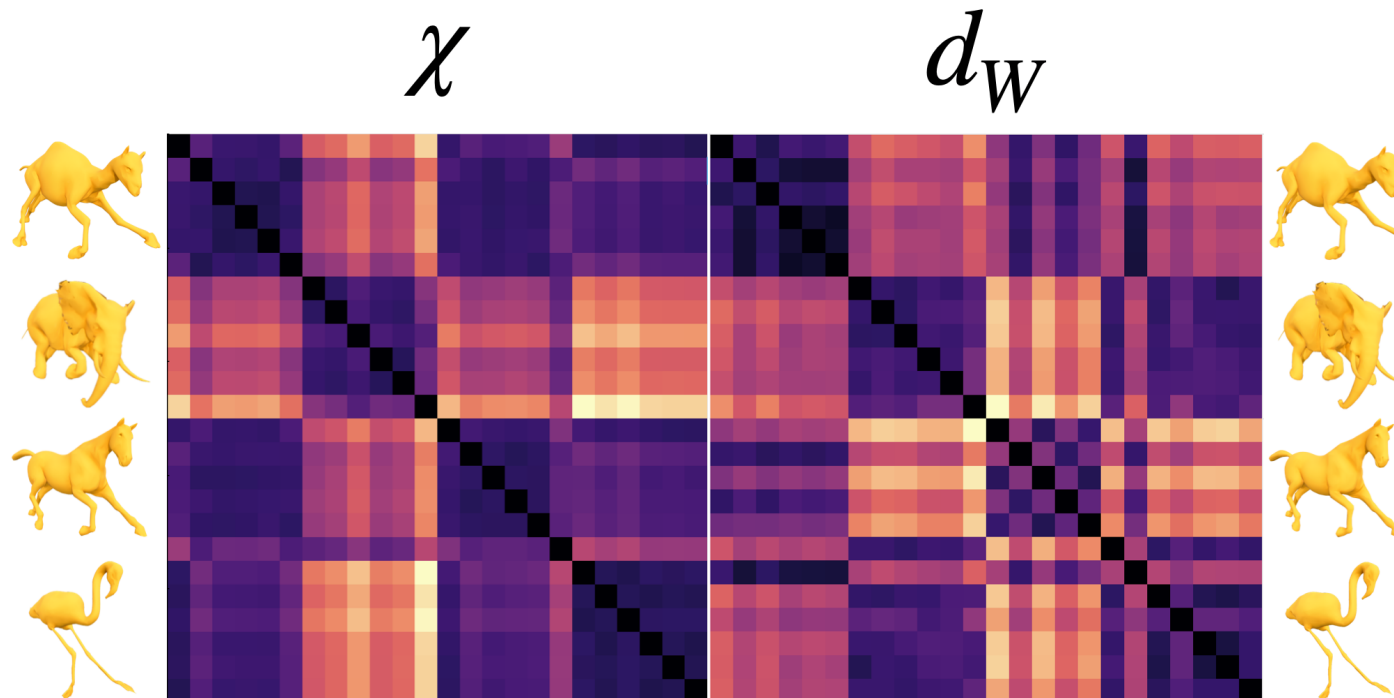


We sample from Δ_+ randomly, retaining signatures with sufficient topological activity

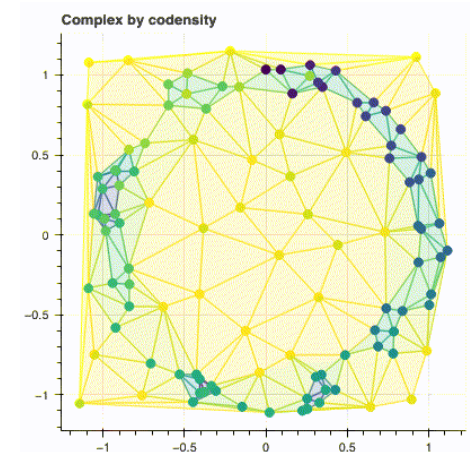
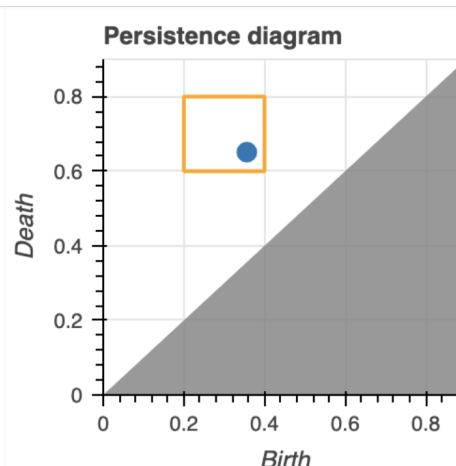
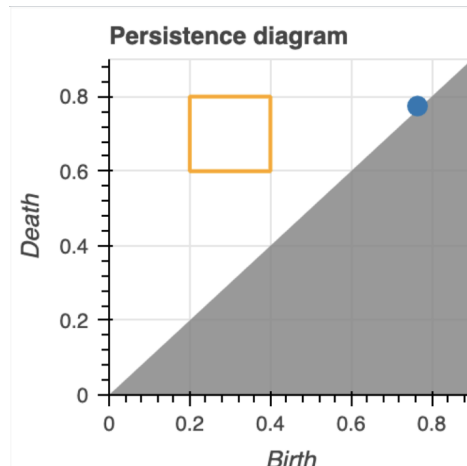
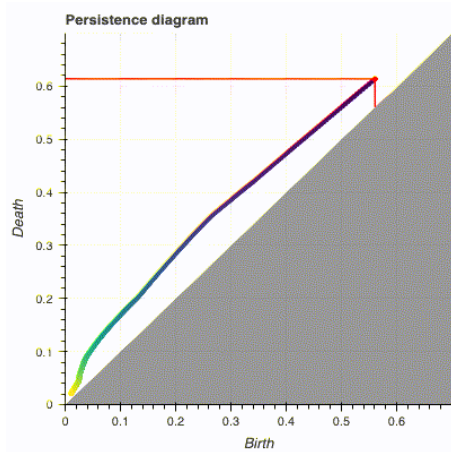
Experiment #2: Intrinsic signatures

...and compared the computed spectral signatures under the relative distance metric:

$$\Lambda(\mu_p^R) = \{\sigma_1, \sigma_2, \dots, \sigma_n\}, \quad \chi(\sigma, \tilde{\sigma}) = \sum_{i=1}^n \frac{|\sigma_i - \tilde{\sigma}_i|}{\sqrt{\sigma_i + \tilde{\sigma}_i}}$$

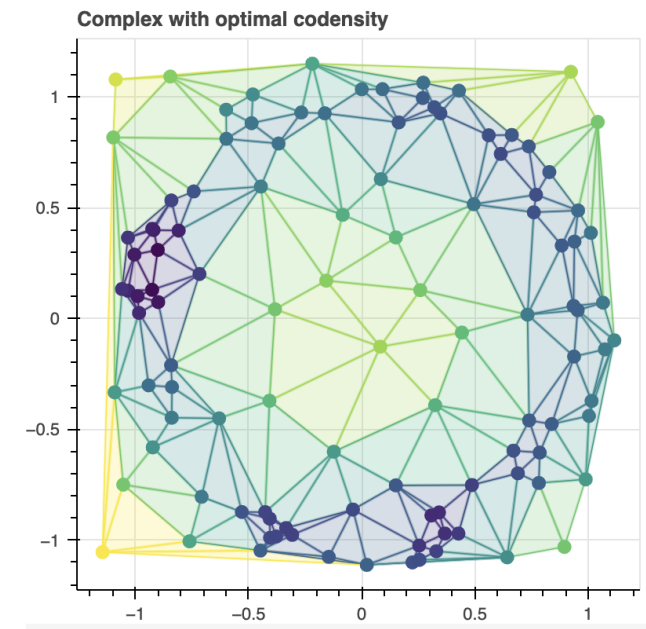
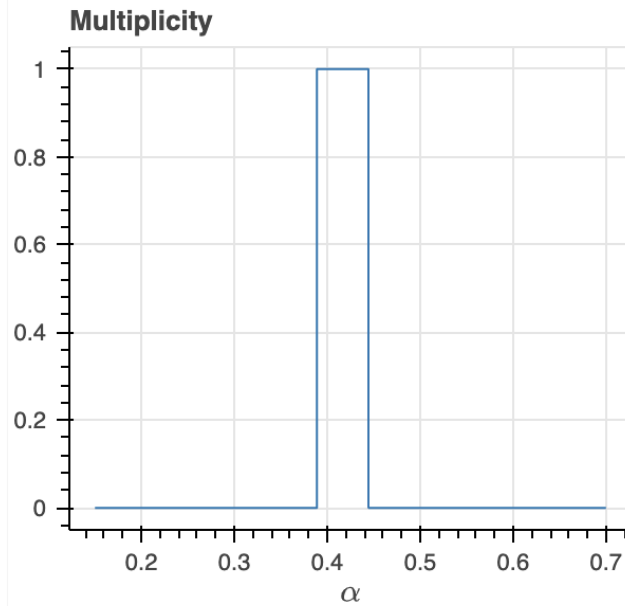
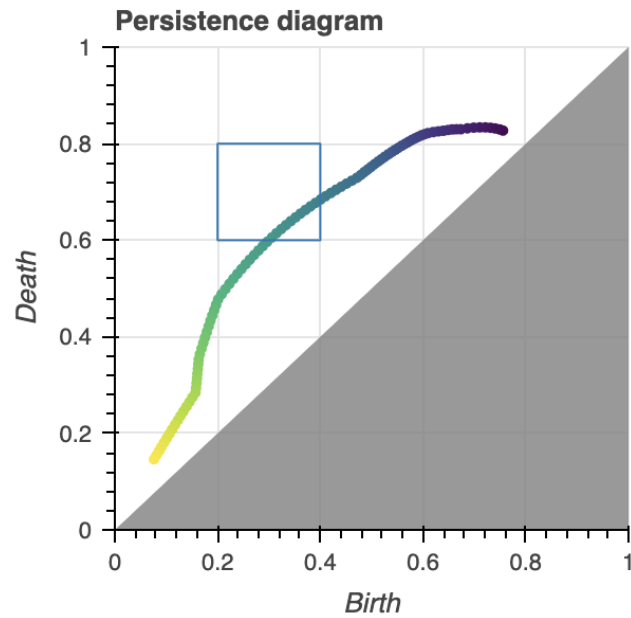


Experiment #3: Filtration optimization



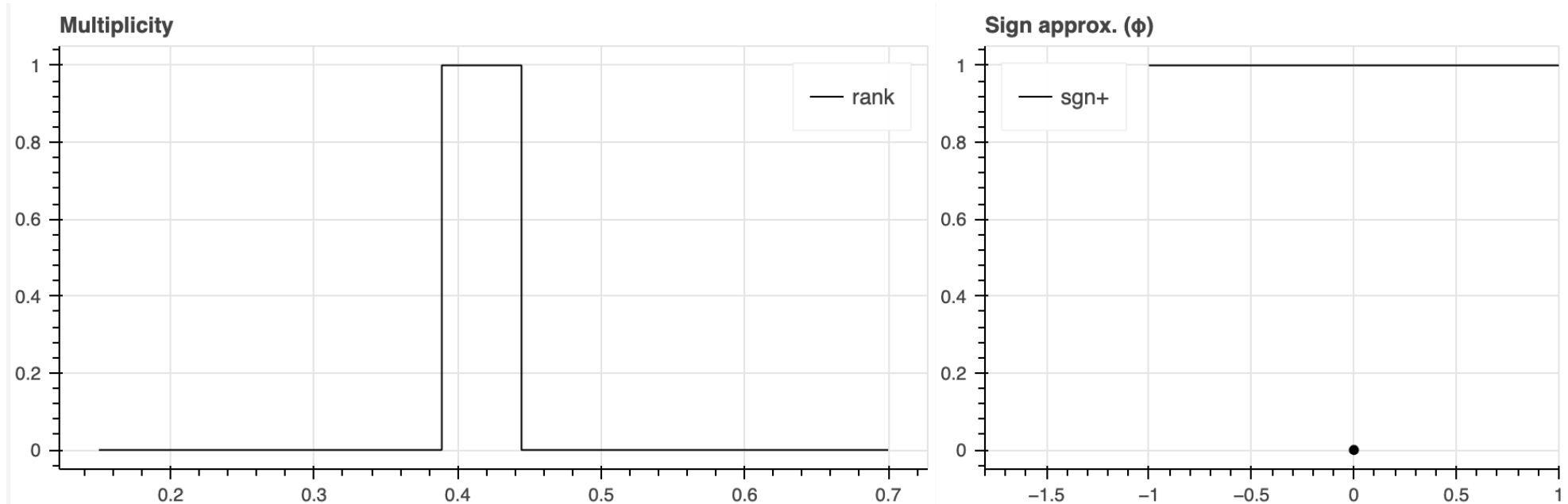
$$\alpha^* = \arg \max_{\alpha \in \mathbb{R}} \text{card}(\text{dgm}(K_\bullet, f_\alpha)|_R)$$

Experiment #3: Filtration optimization



$$\alpha^* = \arg \max_{\alpha \in \mathbb{R}} \text{card}(\text{dgm}(K_\bullet, f_\alpha)|_R)$$

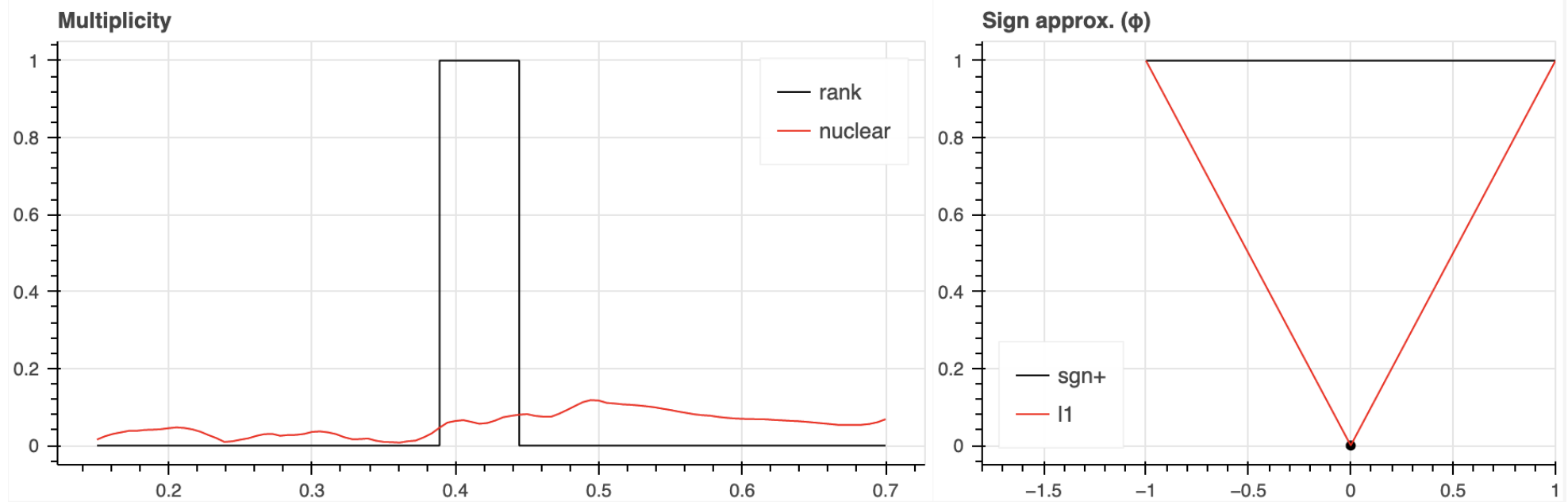
Experiment #3: Filtration optimization



$$\text{rank}(X) = \sum_{i=1}^n \text{sgn}_+(\sigma_i)$$

$$\mu_p^R = \text{rank}(\partial_{p+1}^{j+1,k}) - \text{rank}(\partial_{p+1}^{i+1,k}) - \text{rank}(\partial_{p+1}^{j+1,l}) + \text{rank}(\partial_{p+1}^{i+1,l})$$

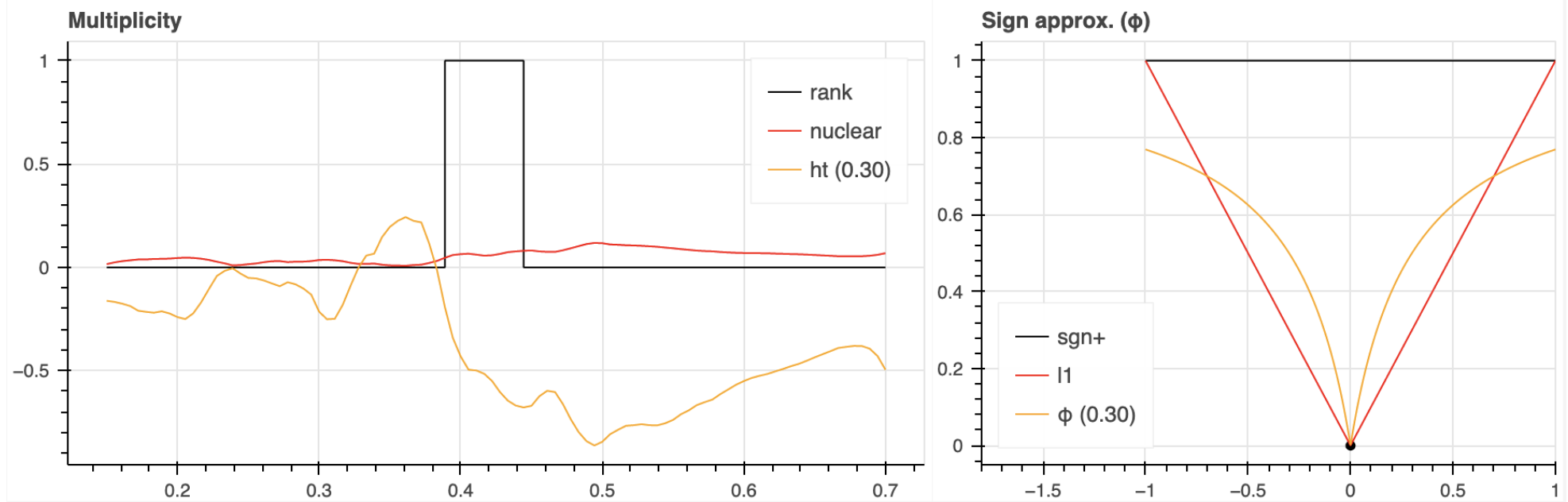
Experiment #3: Filtration optimization



$$\|X\|_* = \sum_{i=1}^n |\sigma_i|$$

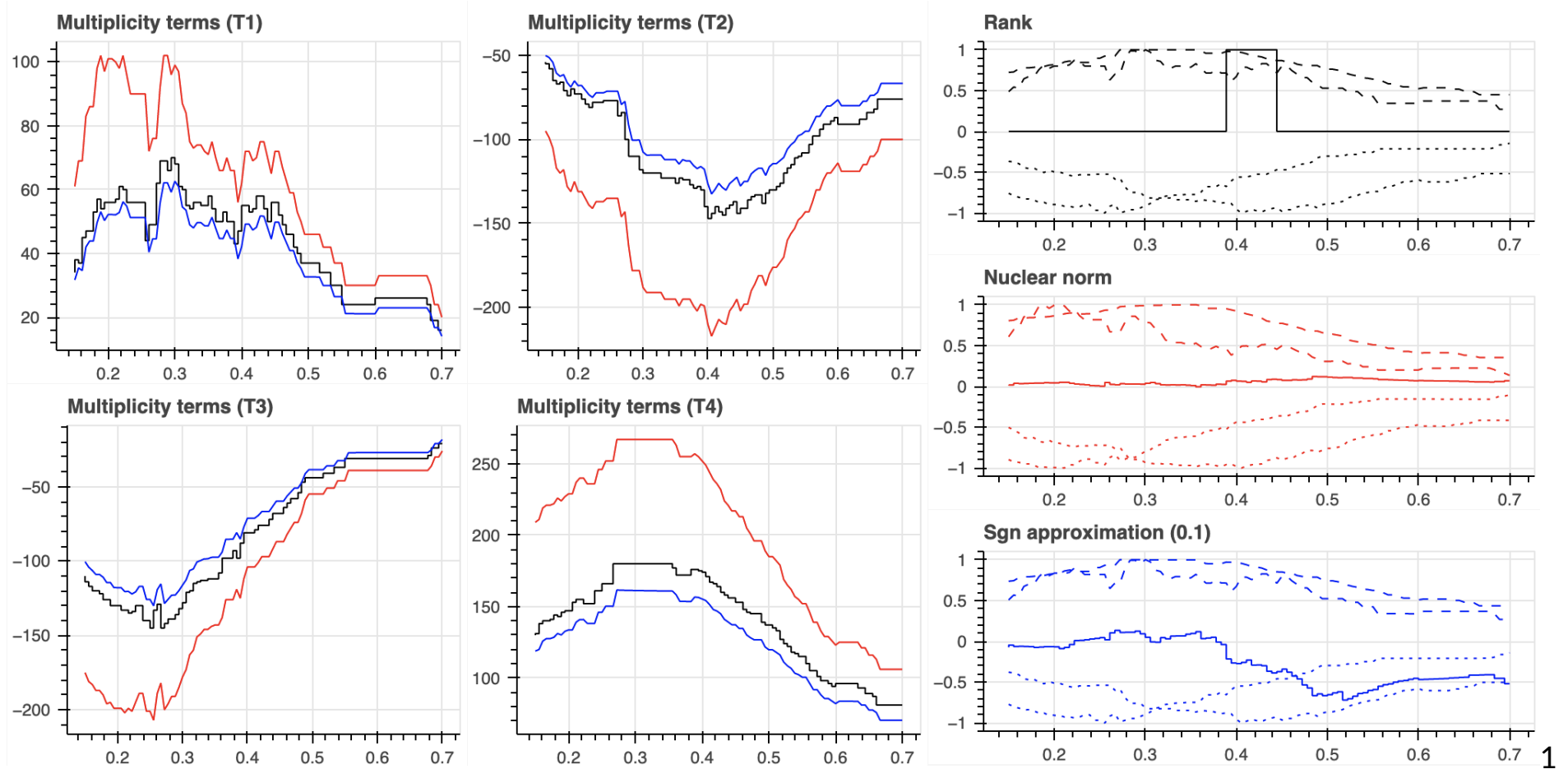
$$\hat{\mu}_p^R = \|\partial_{p+1}^{j+1,k}\|_* - \|\partial_{p+1}^{i+1,k}\|_* - \|\partial_{p+1}^{j+1,l}\|_* + \|\partial_{p+1}^{i+1,l}\|_*$$

Experiment #3: Filtration optimization



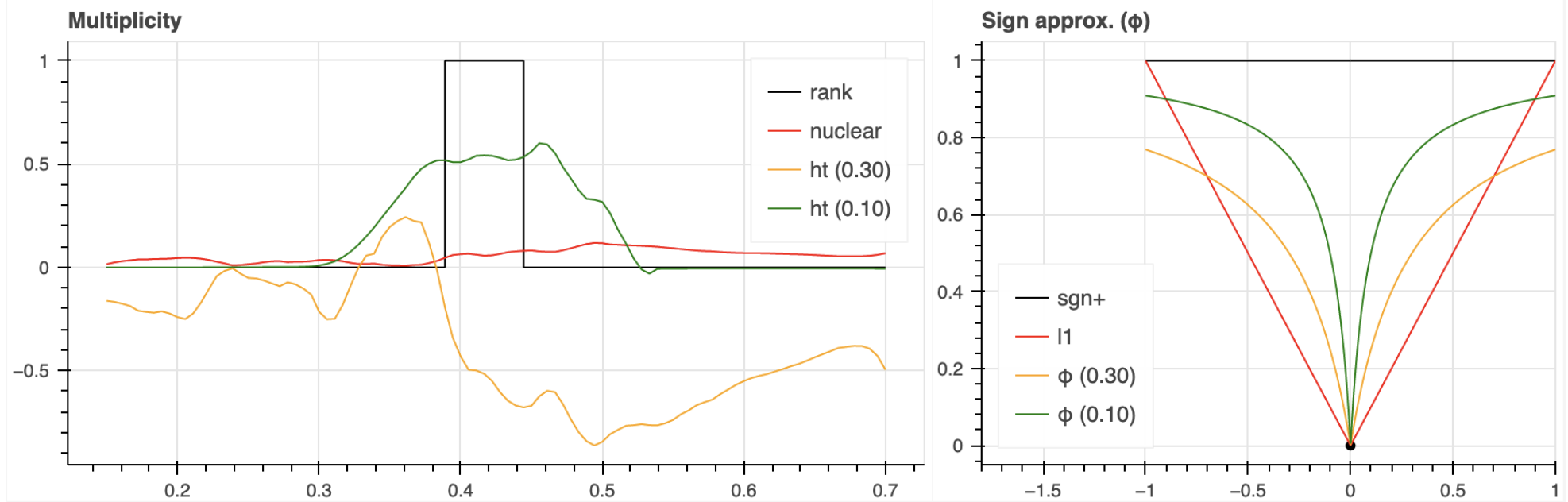
$$\|\Phi_\epsilon(X)\|_* = \sum_{i=1}^n \phi(|\sigma_i|, \epsilon), \quad \epsilon = 0.30$$

Experiment #3: Filtration optimization



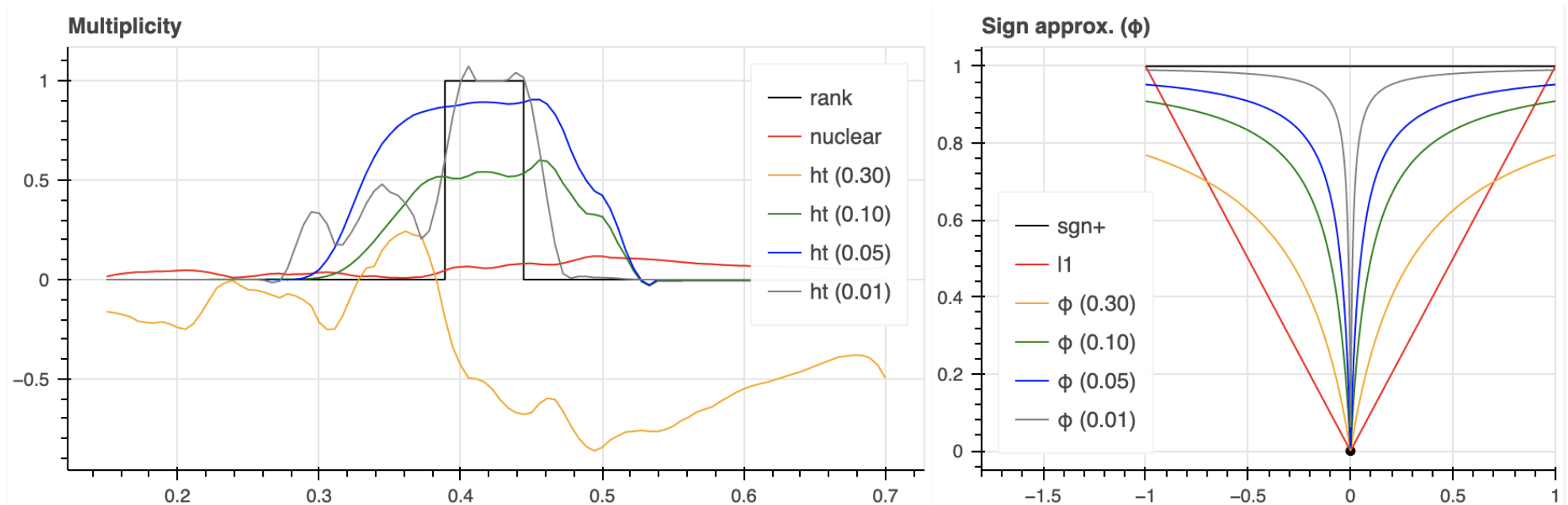
1. Xu, Weiyu, and Babak Hassibi. "Precise Stability Phase Transitions for $\|_1$ Minimization: A Unified Geometric Framework." IEEE transactions on information theory (2011)

Experiment #3: Filtration optimization



$$\|\Phi_\epsilon(X)\|_* = \sum_{i=1}^n \phi(|\sigma_i|, \epsilon), \quad \epsilon = 0.10$$

Experiment #3: Filtration optimization



$$\|\Phi_\epsilon(X)\|_* = \sum_{i=1}^n \phi(|\sigma_i|, \epsilon), \quad \epsilon \rightarrow 0^+$$

Time permitting: Computation

Spectra of Laplacian operators well-studied:

- Iterative Krylov methods / Lanczos dominate solving sparse systems²
- Many laplacian preconditioning methods known ([Jambulapati and Sidford 2021](#))
- Nearly optimal algorithms known for SDD ([Stathopoulos and McCombs 2007](#))

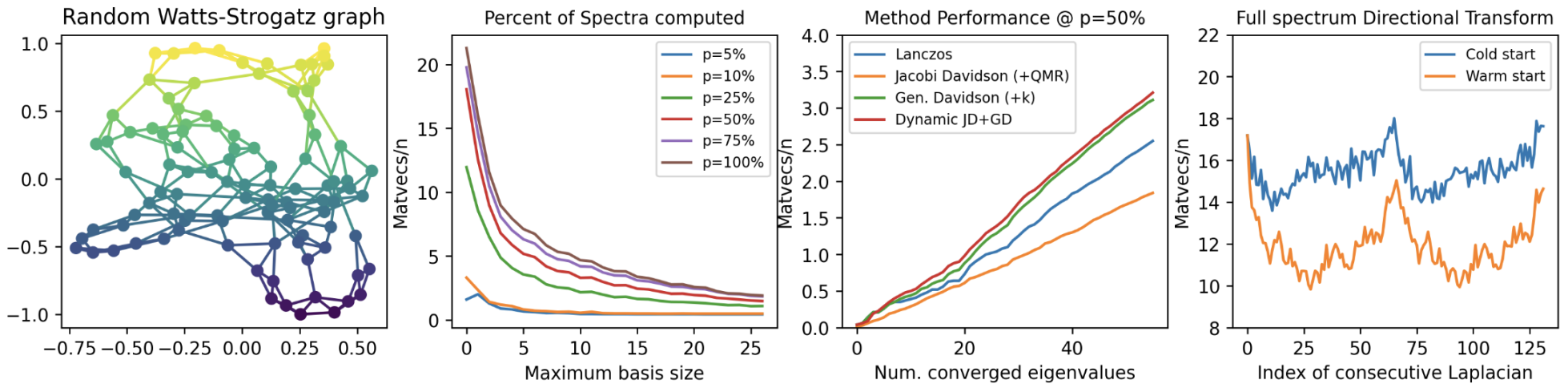
Theorem (Simon 1984): Given a symmetric rank- r matrix $A \in \mathbb{R}^{n \times n}$ whose matrix-vector operator $A \mapsto Ax$ requires $O(\eta)$ time and $O(\nu)$ space, the Lanczos iteration computes $\Lambda(A) = \{\lambda_1, \lambda_2, \dots, \lambda_r\}$ in $O(\max\{\eta, n\} \cdot r)$ time and $O(\max\{\nu, n\})$ space done in exact arithmetic.

- Permutation invariance \implies can optimize memory access of SpMat operation
- Any complex data structure suffices, e.g. tries², combinadics, etc...

See Parlett ([1995](#)) for an overview of the Lanczos. See ([Boissonnat and Maria 2014](#)) for representing complexes.

Time permitting: Computation

Preliminary experiments suggest the scalability is promising



- $\approx \leq 25$ Lanczos vectors to approximate full spectrum at $\epsilon > 0$
- $\implies O(n)$ memory to obtain $\|\cdot\|_*$ in $O(n^2)$ time (with small constants!)
- Larger values ϵ or lower numerical tolerances \implies essentially linear time compute
- Previously computed eigenvectors can be re-used for “warm restarts”

Conclusion

Spectral relaxation of rank invariant using Löwner operators

- Suitable for parameterized families of filtrations
- Differentiable + amenable for optimization
- Stable to perturbations in f_α when $\epsilon > 0$, but unstable as $\epsilon \rightarrow 0^+$
- Excellent compute properties. Implementation ongoing.
- Better optimizer implementation also ongoing.

Looking for collaborators! In particular:

- Optimizing parameterized filtrations
- Differentiating n-parameter families of filtrations
- Encoding features with Laplacian spectra
- Sparse minimization problems (compressive sensing)
- Understanding connections to other areas of math

References

- Adams, Henry, Tegan Emerson, Michael Kirby, Rachel Neville, Chris Peterson, Patrick Shipman, Sofya Chepushtanova, Eric Hanson, Francis Motta, and Lori Ziegelmeier. 2017. "Persistence Images: A Stable Vector Representation of Persistent Homology." *Journal of Machine Learning Research* 18.
- Anderson Jr, William N, and Richard James Duffin. 1969. "Series and Parallel Addition of Matrices." *Journal of Mathematical Analysis and Applications* 26 (3): 576–94.
- Bauer, Ulrich, Talha Bin Masood, Barbara Giunti, Guillaume Houry, Michael Kerber, and Abhishek Rathod. 2022. "Keeping It Sparse: Computing Persistent Homology Revised." *arXiv Preprint arXiv:2211.09075*.
- Bauschke, Heinz H, Patrick L Combettes, et al. 2011. *Convex Analysis and Monotone Operator Theory in Hilbert Spaces*. Vol. 408. Springer.
- Ben-Israel, Adi. 1967. "On the Geometry of Subspaces in Euclidean n-Spaces." *SIAM Journal on Applied Mathematics* 15 (5): 1184–98.
- . 2015. "Projectors on Intersection of Subspaces." *Contemporary Mathematics* 636: 41–50.
- Bhatia, Rajendra. 2013. *Matrix Analysis*. Vol. 169. Springer Science & Business Media.
- Bi, Shujun, Le Han, and Shaohua Pan. 2013. "Approximation of Rank Function and Its Application to the Nearest Low-Rank Correlation Matrix." *Journal of Global*

- Optimization 57 (4): 1113–37.
- Boissonnat, Jean-Daniel, and Clément Maria. 2014. “The Simplex Tree: An Efficient Data Structure for General Simplicial Complexes.” *Algorithmica* 70: 406–27.
- Bubenik, Peter. 2020. “The Persistence Landscape and Some of Its Properties.” In *Topological Data Analysis: The Abel Symposium 2018*, 97–117. Springer.
- Cerri, Andrea, Barbara Di Fabio, Massimo Ferri, Patrizio Frosini, and Claudia Landi. 2013. “Betti Numbers in Multidimensional Persistent Homology Are Stable Functions.” *Mathematical Methods in the Applied Sciences* 36 (12): 1543–57.
- Chazal, Frédéric, David Cohen-Steiner, Leonidas J Guibas, Facundo Mémoli, and Steve Y Oudot. 2009. “Gromov-Hausdorff Stable Signatures for Shapes Using Persistence.” In *Computer Graphics Forum*, 28:1393–403. 5. Wiley Online Library.
- Chazal, Frédéric, Vin De Silva, Marc Glisse, and Steve Oudot. 2016. *The Structure and Stability of Persistence Modules*. Vol. 10. Springer.
- Chen, Chao, and Michael Kerber. 2011. “An Output-Sensitive Algorithm for Persistent Homology.” In *Proceedings of the Twenty-Seventh Annual Symposium on Computational Geometry*, 207–16.
- Dey, Tamal K, Woojin Kim, and Facundo Mémoli. 2021. “Computing Generalized Rank Invariant for 2-Parameter Persistence Modules via Zigzag Persistence and Its Applications.” *arXiv Preprint arXiv:2111.15058*.
- Dey, Tamal Krishna, and Yusu Wang. 2022. *Computational Topology for Data Analysis*. Cambridge University Press.

- Edelsbrunner, Herbert, David Letscher, and Afra Zomorodian. 2000. “Topological Persistence and Simplification.” In *Proceedings 41st Annual Symposium on Foundations of Computer Science*, 454–63. IEEE.
- Horak, Danijela, and Jürgen Jost. 2013. “Spectra of Combinatorial Laplace Operators on Simplicial Complexes.” *Advances in Mathematics* 244: 303–36.
- Jambulapati, Arun, and Aaron Sidford. 2021. “Ultrasparse Ultrasparsifiers and Faster Laplacian System Solvers.” In *Proceedings of the 2021 ACM-SIAM Symposium on Discrete Algorithms (SODA)*, 540–59. SIAM.
- Jiang, Tianpei, and Hristo Sendov. 2018. “A Unified Approach to Operator Monotone Functions.” *Linear Algebra and Its Applications* 541: 185–210.
- Kim, Kwangho, Jisu Kim, Manzil Zaheer, Joon Kim, Frédéric Chazal, and Larry Wasserman. 2020. “Pllay: Efficient Topological Layer Based on Persistent Landscapes.” *Advances in Neural Information Processing Systems* 33: 15965–77.
- Komzsik, Louis. 2003. *The Lanczos Method: Evolution and Application*. SIAM.
- McCleary, Alexander, and Amit Patel. 2022. “Edit Distance and Persistence Diagrams over Lattices.” *SIAM Journal on Applied Algebra and Geometry* 6 (2): 134–55.
- Mémoli, Facundo. 2012. “Some Properties of Gromov–Hausdorff Distances.” *Discrete & Computational Geometry* 48: 416–40.
- Mémoli, Facundo, Zhengchao Wan, and Yusu Wang. 2022. “Persistent Laplacians: Properties, Algorithms and Implications.” *SIAM Journal on Mathematics of Data Science* 4 (2): 858–84.

- Parlett, Beresford N. 1995. “Do We Fully Understand the Symmetric Lanczos Algorithm Yet?” CALIFORNIA UNIV BERKELEY DEPT OF MATHEMATICS.
- Piekenbrock, Matthew, and Jose A Perea. 2021. “Move Schedules: Fast Persistence Computations in Coarse Dynamic Settings.” *arXiv Preprint arXiv:2104.12285*.
- Simon, Horst D. 1984. “Analysis of the Symmetric Lanczos Algorithm with Reorthogonalization Methods.” *Linear Algebra and Its Applications* 61: 101–31.
- Som, Anirudh, Hongjun Choi, Karthikeyan Natesan Ramamurthy, Matthew P Buman, and Pavan Turaga. 2020. “Pi-Net: A Deep Learning Approach to Extract Topological Persistence Images.” In *Proceedings of the IEEE/CVF Conference on Computer Vision and Pattern Recognition Workshops*, 834–35.
- Stathopoulos, Andreas, and James R McCombs. 2007. “Nearly Optimal Preconditioned Methods for Hermitian Eigenproblems Under Limited Memory. Part II: Seeking Many Eigenvalues.” *SIAM Journal on Scientific Computing* 29 (5): 2162–88.
- Zomorodian, Afra, and Gunnar Carlsson. 2004. “Computing Persistent Homology.” In *Proceedings of the Twentieth Annual Symposium on Computational Geometry*, 347–56.

